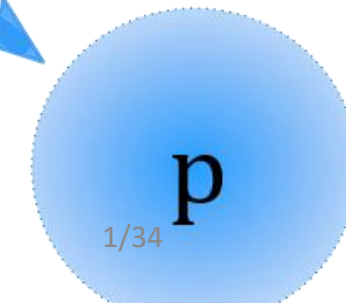
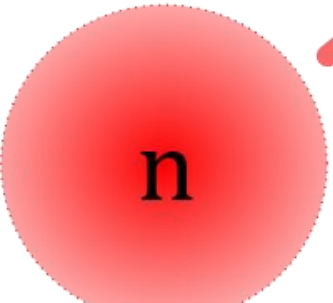


Path from Lattice QCD to Neutrinoless  
Double-Beta Decay Amplitude  
Saurabh Kadam  
with  
Zohreh Davoudi  
PRD 102, 114521 (2020)  
PRL 126, 152003 (2021)  
PRD 105, 094502 (2022)



# Outline

## □ Motivation

Why is it needed?

## □ Formalism

What are the tools?

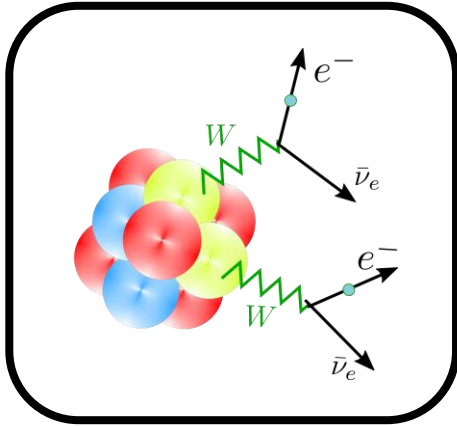
## □ Results

How to use them?

# Double $\beta$ Decays

## Two neutrino double beta decay ( $2\nu\beta\beta$ )

Eugene Wigner,  
Goeppert-Mayer  
(1935)

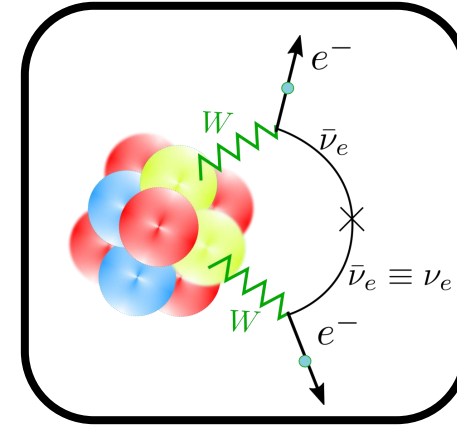


- Standard model (SM) process
- Extremely rare and has been observed

$$T_{1/2}(2\nu\beta\beta) \sim 10^{20}y$$

## Neutrinoless double beta decay ( $0\nu\beta\beta$ )

Racah (1937)  
Furry (1939)



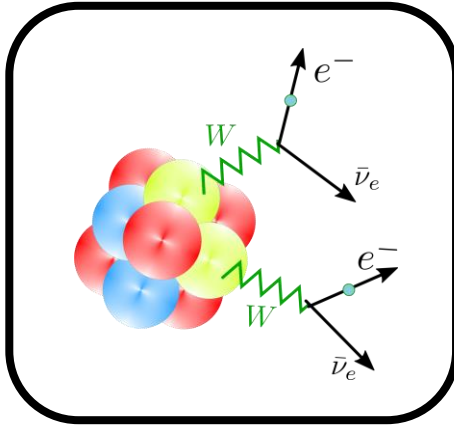
- Total lepton number is violated
- Beyond the standard model (BSM) process
- Searches for it are ongoing
- Neutrinos are their own anti-particles

Avignone, Elliott and Engel  
Reviews of Modern Physics, 80 (2008)

# Double $\beta$ Decays

## Two neutrino double beta decay ( $2\nu\beta\beta$ )

Eugene Wigner,  
Goeppert-Mayer  
(1935)



- Standard model (SM) process
- Extremely rare and has been observed

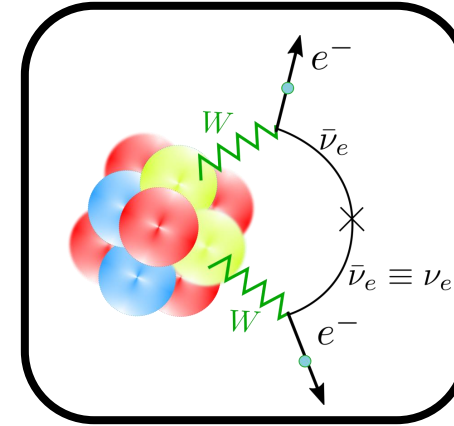
$$T_{1/2}(2\nu\beta\beta) \sim 10^{20}y$$

- Dominant background for  $0\nu\beta\beta$  search experiments
- $2\nu\beta\beta$  can also probe potential BSM scenarios

Deppisch, Graf, and Šimkovic  
PhysRevLett.125.171801

## Neutrinoless double beta decay ( $0\nu\beta\beta$ )

Racah (1937)  
Furry (1939)



- Total lepton number is violated
- Beyond the standard model (BSM) process
- Searches for it are ongoing
- Neutrinos are their own anti-particles

Avignone, Elliott and Engel  
Reviews of Modern Physics, 80 (2008)

# What can possibly be responsible for a $0\nu\beta\beta$ decay?

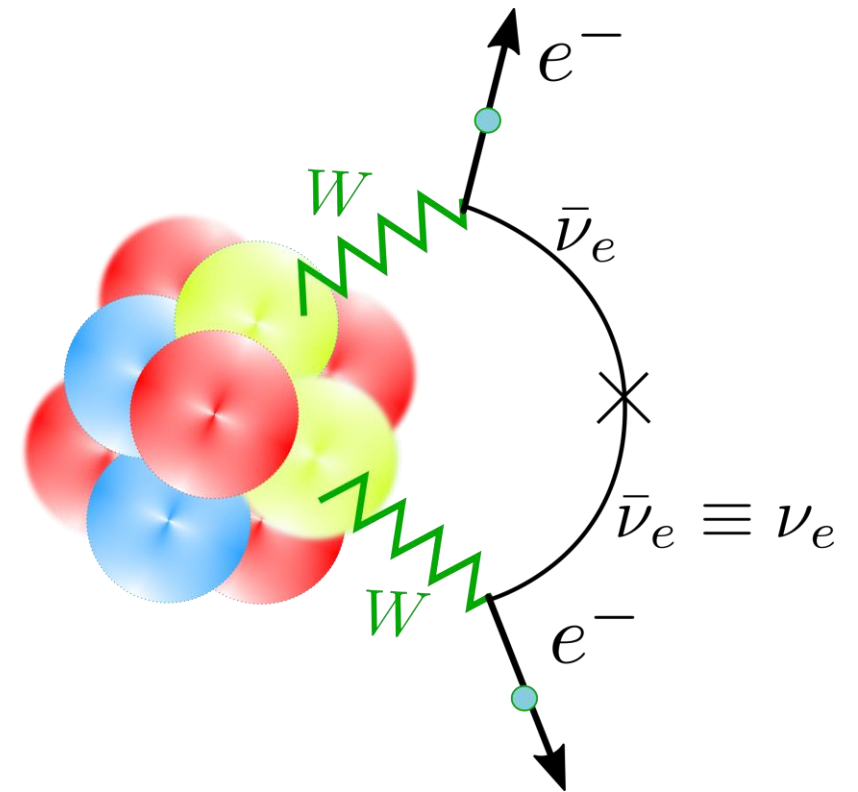
- Minimal deviation from the SM:

Light neutrino exchange scenario

- SM neutrinos are promoted to Majorana neutrinos
- Effective Majorana mass

$$m_{\beta\beta} = \sum_k m_k U_{ek}^2$$

Needs accurate constraints



# Obtaining Effective Majorana Mass from Experiments

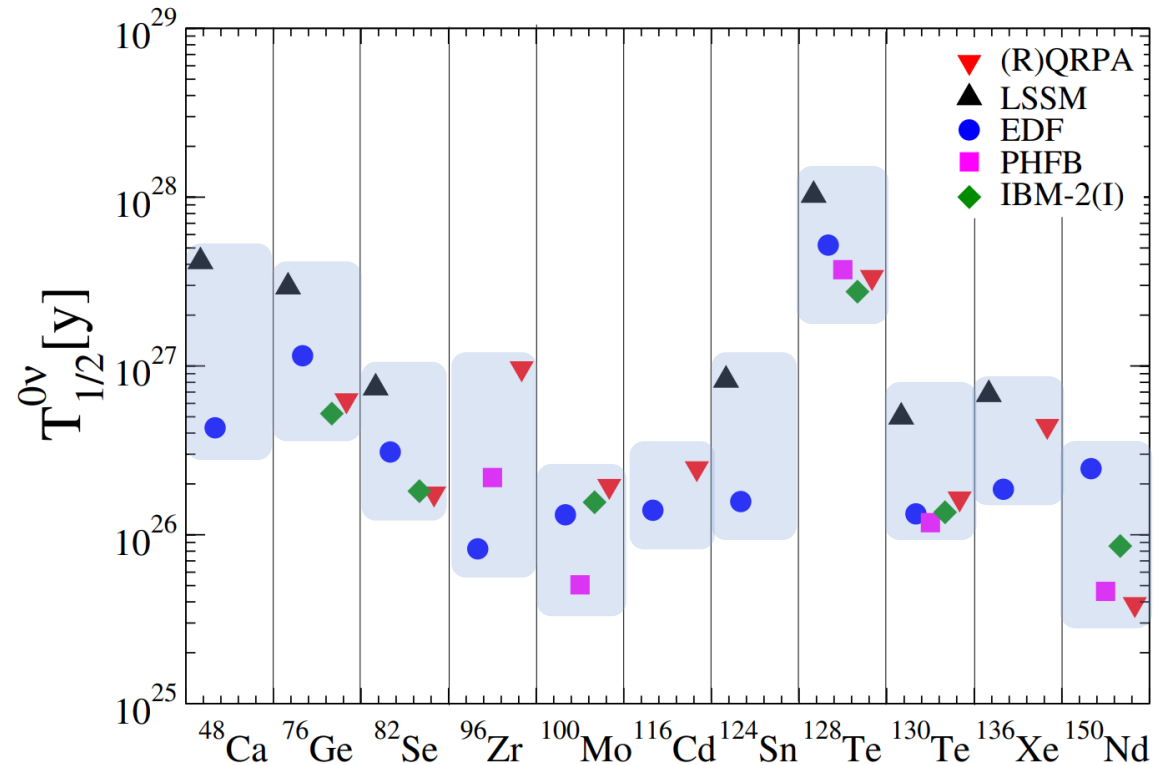
Phase space factor

$$(T_{1/2}^{0\nu})^{-1} = G_{0\nu}(Q_{\beta\beta}, Z) |M_{0\nu}|^2 \langle m_{\beta\beta} \rangle^2$$

Nuclear Matrix Element (NME)  
in Light Neutrino Exchange  
Scenario

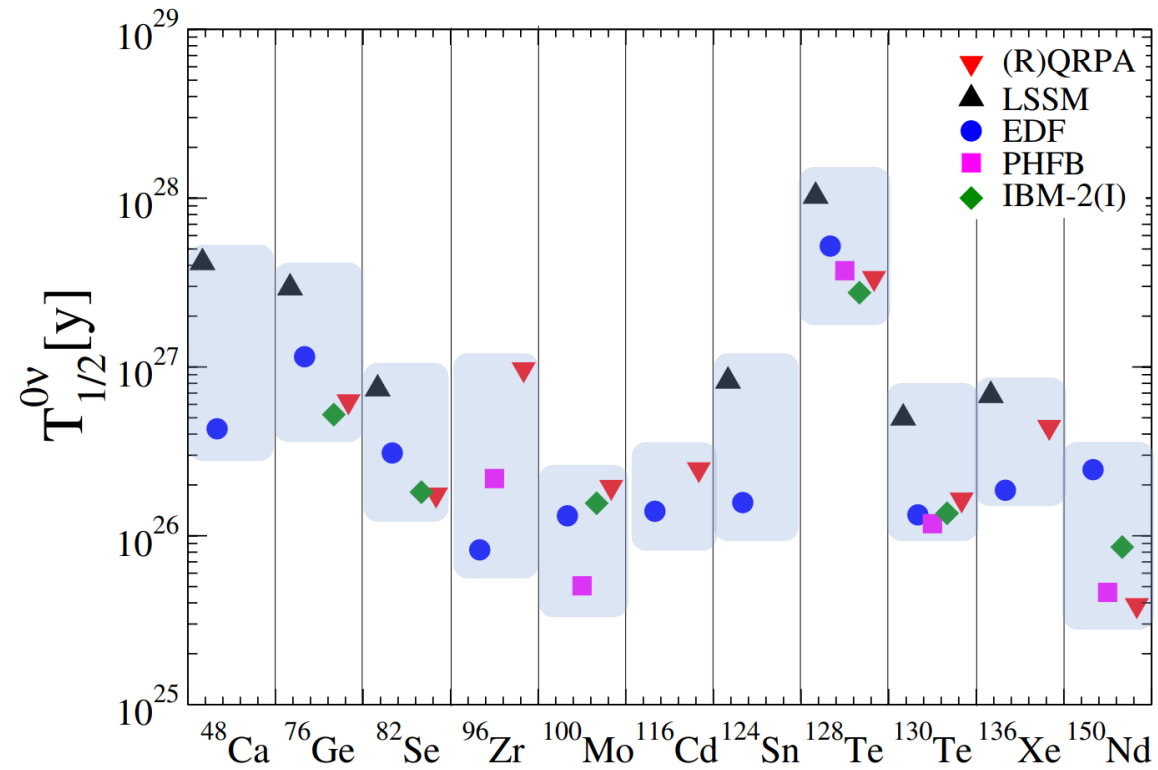
Half-lives from different methods for NME calculations

$$\langle m_{\beta\beta} \rangle = 0.05 \text{ eV}$$

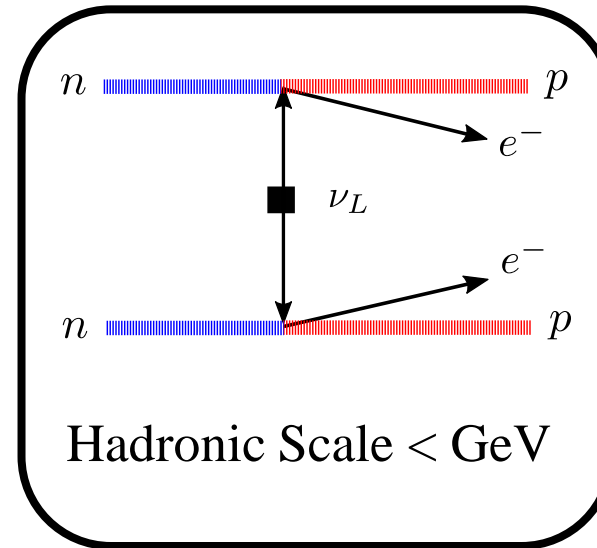


Vergados, Ejiri and Simkovic,  
Rep. Prog. Phys. 75 106301 (2012)

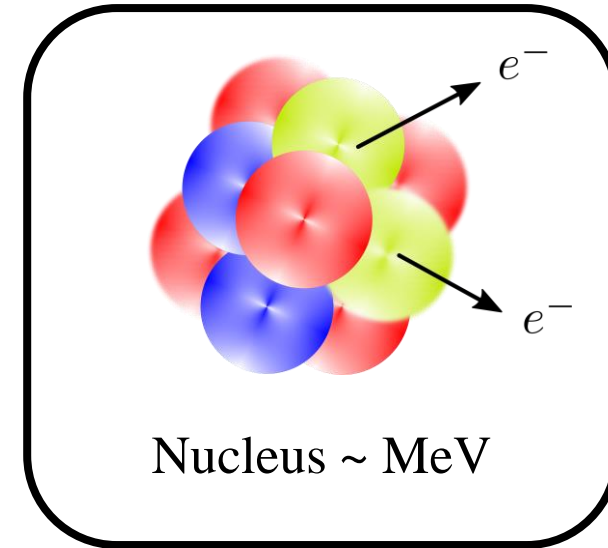
# What is the source of these uncertainties in NME?



# Nuclear Matrix Elements



Nuclear EFT



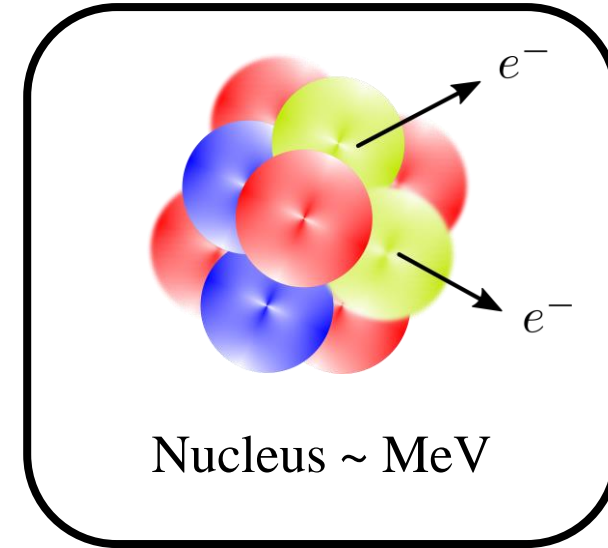
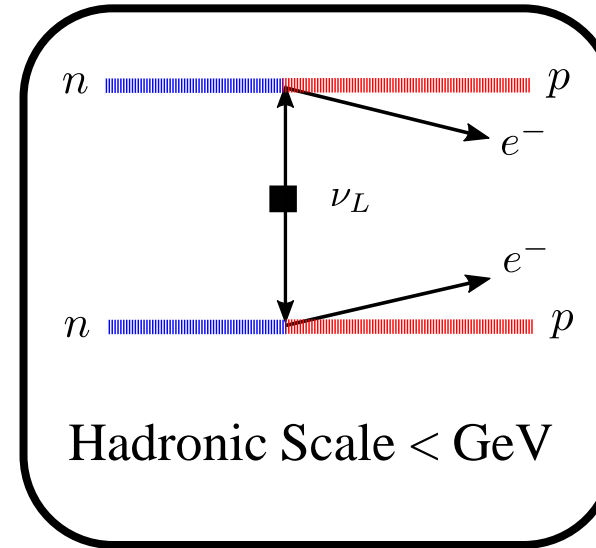
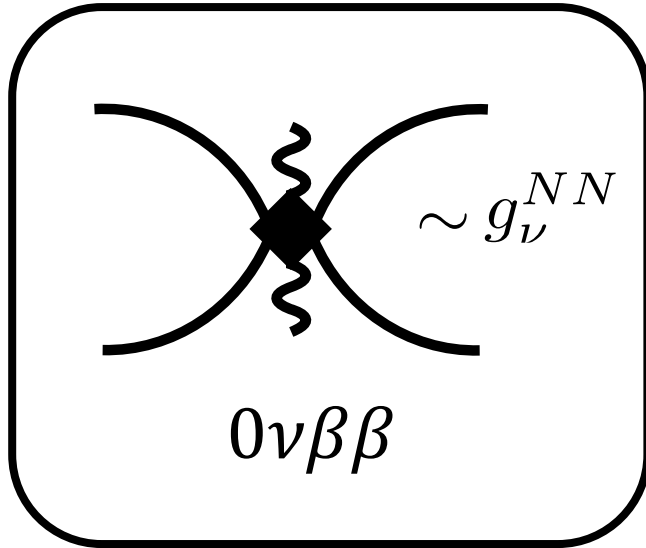
Nuclear Many-Body  
Calculation



# Low Energy Constants (LECs)

# Nuclear Matrix Elements

Cirigliano, Dekens, de Vries, Hoferichter, Mereghetti  
 Phys. Rev. Lett. 126, 172002 (2021)



- Undertermined LEC  $g_{\nu}^{NN}$  in pionless EFT
- LO  $0\nu\beta\beta$  amplitude remains unknown
- An indirect estimate of  $g_{\nu}^{NN}$  suggests an

enhancement of  $\sim 40\%$  in NME for Ca nucleus

Cirigliano, Dekens, de Vries, Hoferichter, Mereghetti  
 Phys. Rev. Lett. 126, 172002

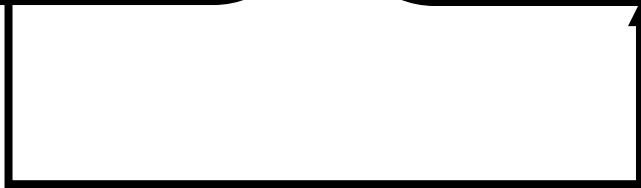
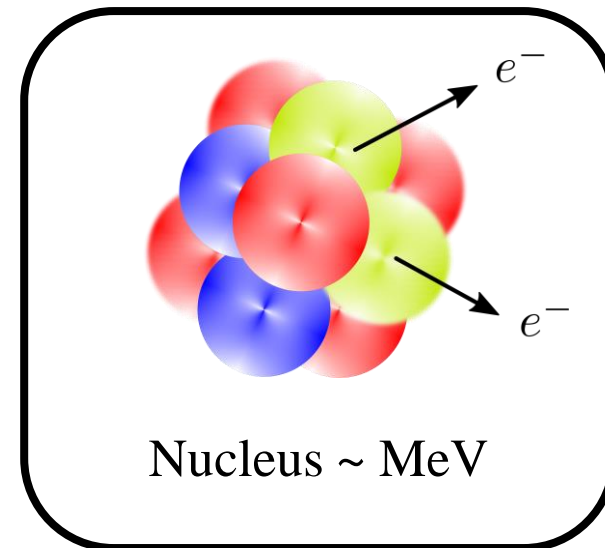
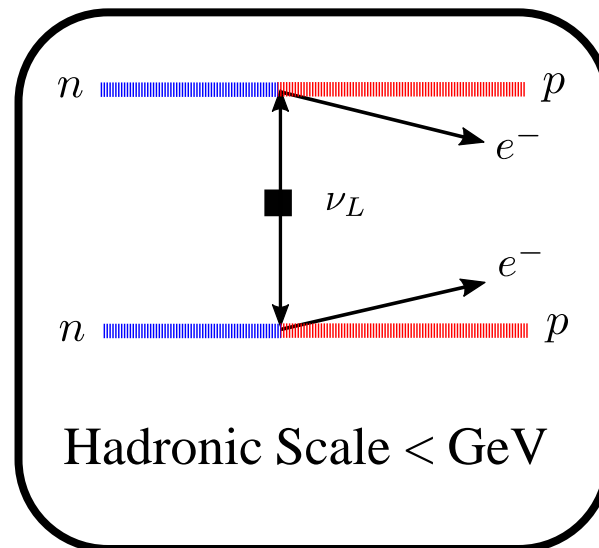
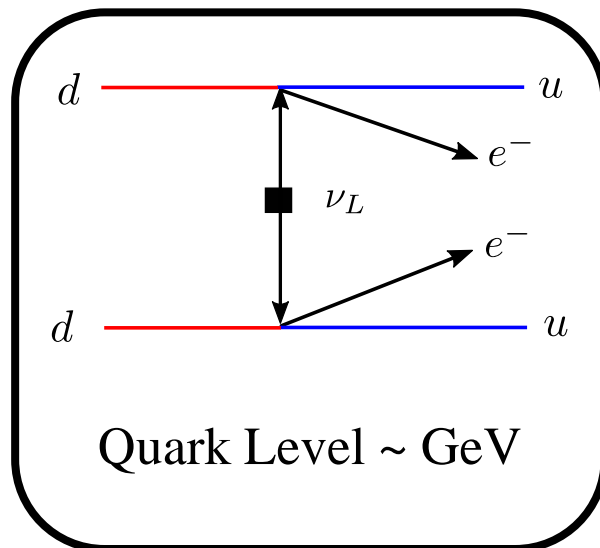
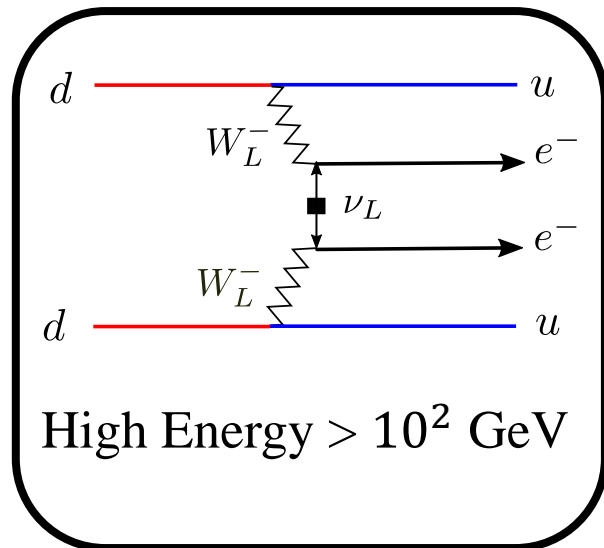
Wirth, Yao, Hergert  
 PhysRevLett.127.242502 (2021)

Jokiniemi, Soriano, Menendez  
 j.physletb.2021.136720 (2021)

Nuclear EFT

Nuclear Many-Body Calculation

# Nuclear Matrix Elements

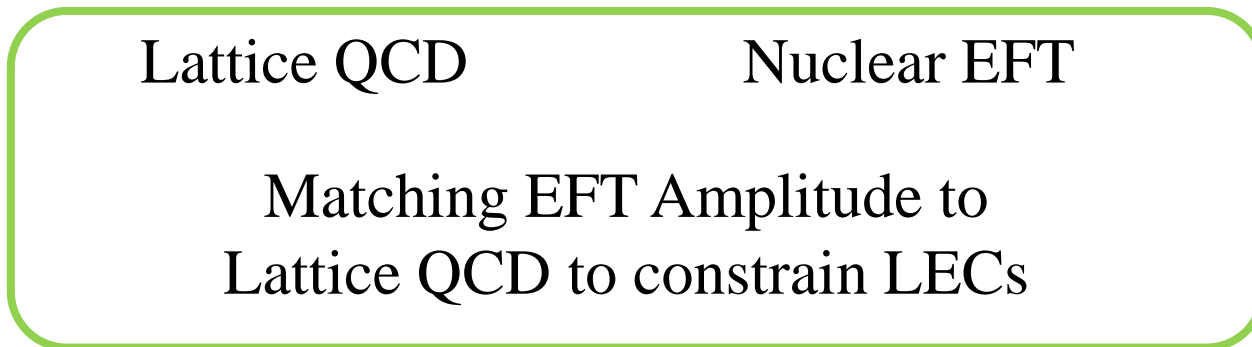
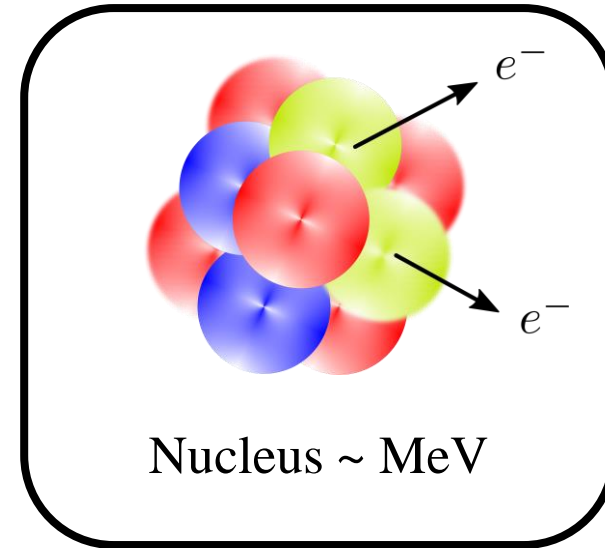
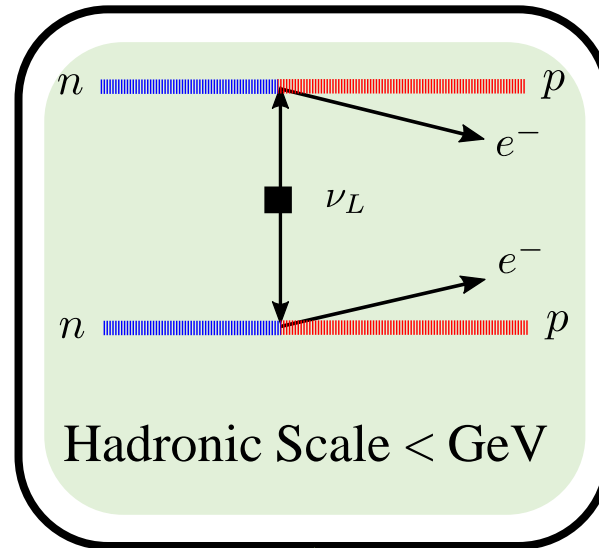
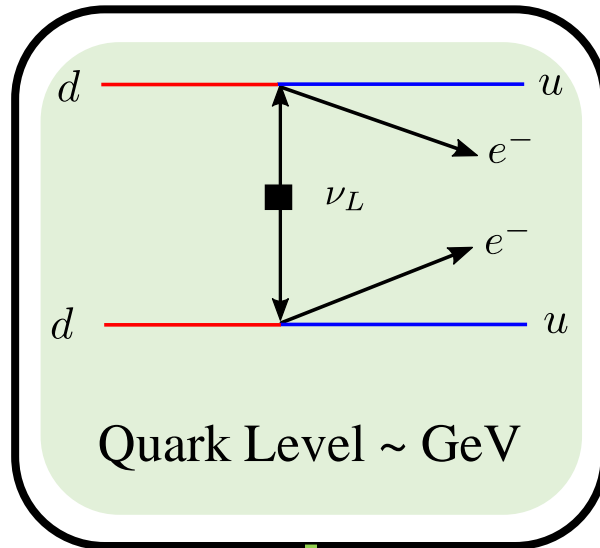
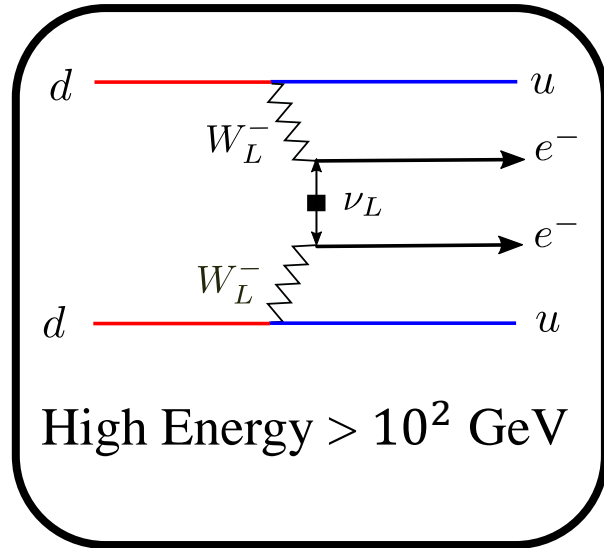


Lattice QCD

Nuclear EFT

Nuclear Many-Body  
Calculation

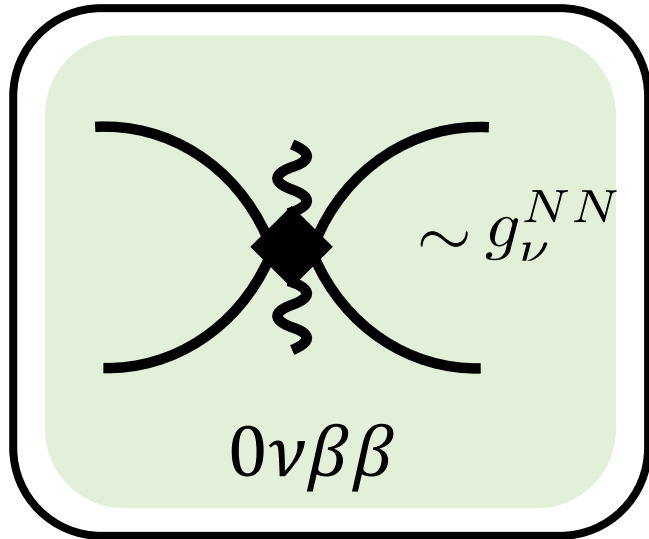
# Nuclear Matrix Elements



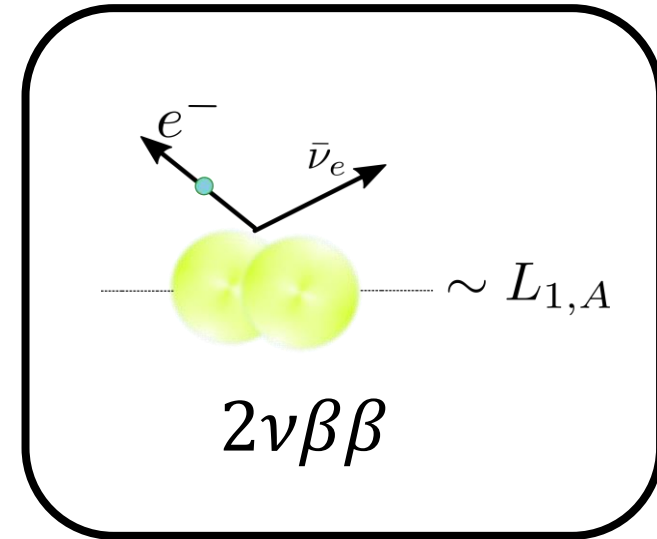
Nuclear Many-Body  
Calculation

Snowmass:  
Ovbb: A Roadmap for Matching  
Theory to Experiment  
arXiv:2203.12169

# Constraining LECs from Lattice QCD



Davoudi and Kadam  
Phys. Rev. Lett. 126, 152003 (2021)



Davoudi and Kadam  
Phys. Rev. D 102, 114521 (2020)

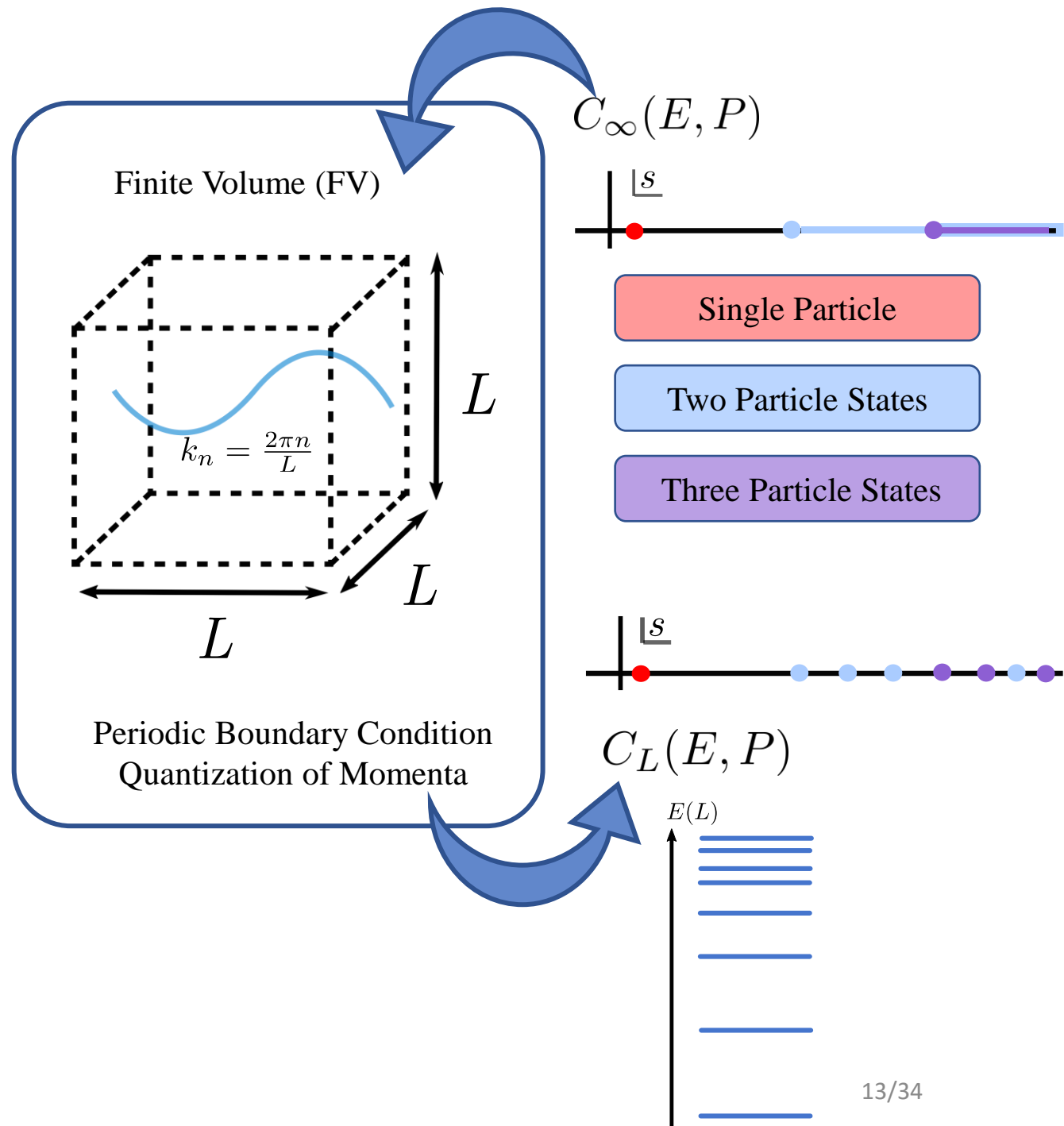
# Lattice QCD

QCD Formulated on

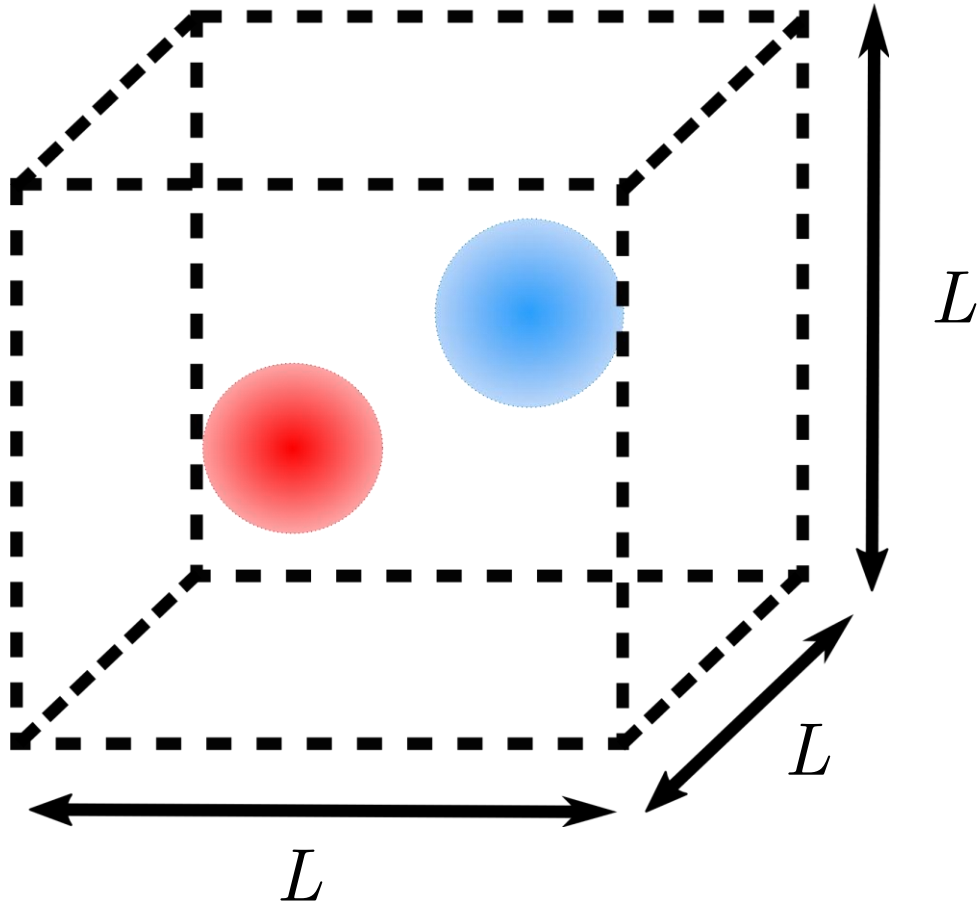
- ❖ Discrete Euclidean Spacetime Grid
- ❖ Lattice spacing  $a$
- ❖ Finite Volume  $L^3$
- ❖ Monte-Carlo Sampling

## Finite vs. Infinite Volume Physics

- ❖ Branch cuts are replaced with poles
- ❖ Corresponding energies give the FV spectrum
- ❖ Position of poles is related to the scattering amplitude



# Assumptions



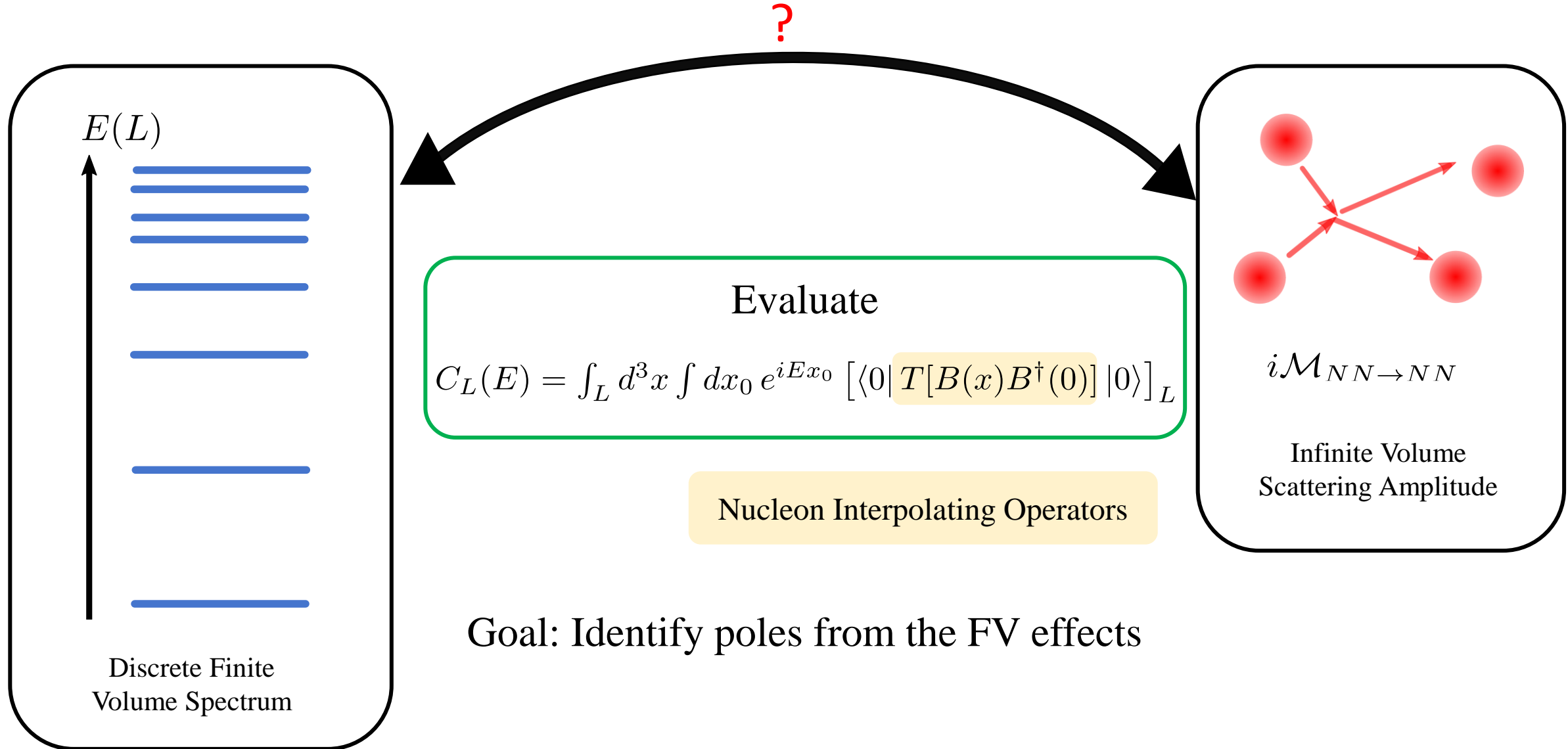
- Lattice spacing  $a \rightarrow 0$
- Ignore discretization effects

- Infinite temporal extent
- Energy is a continuous variable

- In COM frame  $P = (E, \mathbf{0})$
- Energy below three particle threshold

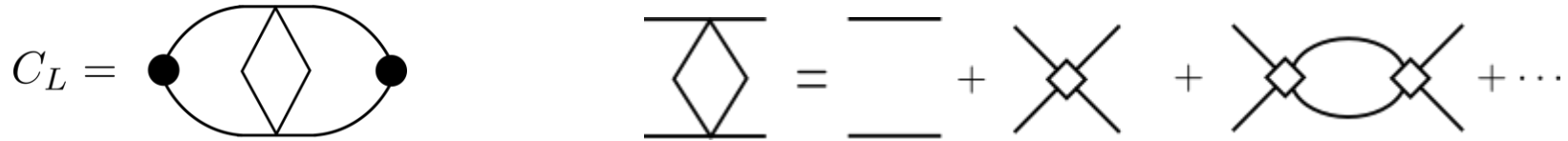


# Two Nucleon Scattering Amplitude



$$C_L(E) = \int_L d^3x \int dx_0 e^{iEx_0} [\langle 0 | T[B(x)B^\dagger(0)] | 0 \rangle]_L$$

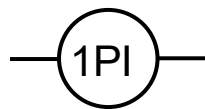
Evaluate the  
correlation function  
non-perturbatively



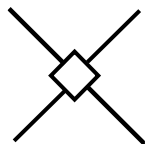
Which diagrams give singular sums in  $\vec{k}$  ?  
If particles in summed loops can go on-shell

Same as Infinite Volume

One particle irreducible diagrams

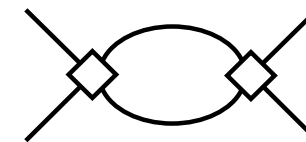


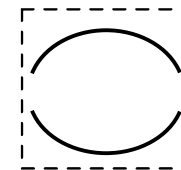
2 → 2 Bethe-Salpeter Kernel



Power Law Difference

Two particle loop in s - channel



  $\sim I_0^V(E) = I_0^\infty(E) + F_0(E)$

Poles in  $C_L(E)$  are identified using  $F_0(E)$



# FV method

Lellouch, and Luscher (LL) (2001),  
Commun. Math. Phys. 219,

Kim, Sachrajda, and Sharpe  
(2005), Nucl. Phys. B727

$$C_L(E) = \int_L d^3x \int dx_0 e^{iEx_0} [\langle 0 | T[B(x)B^\dagger(0)] | 0 \rangle]_L$$

Evaluate the correlation function in EFT non-perturbatively

$$C_L = \text{diagram} \quad \text{diagram} = \text{diagram} + \text{diagram} + \text{diagram} + \dots$$

Identify and isolate FV corrections

$$\text{diagram} \quad \text{diagram} \sim I_0^V(E) = I_0^\infty(E) + F_0(E)$$

Rearrange to get Infinite volume  $2 \rightarrow 2$  amplitude

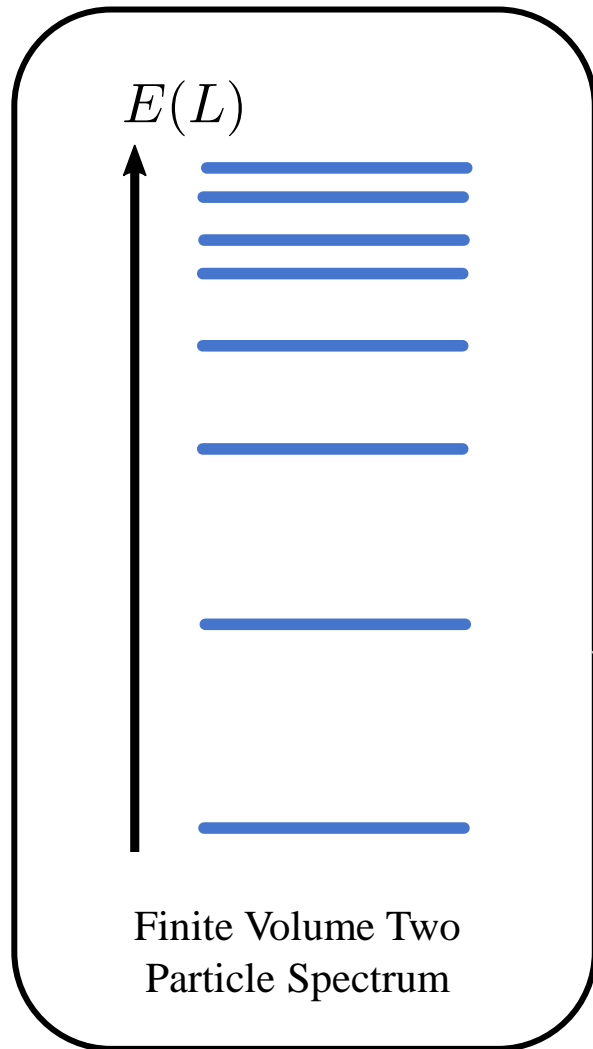
$$C_L = \text{diagram} + \text{diagram} + \dots + \text{diagram} + \text{diagram} + \dots + \text{diagram} + \text{diagram} + \dots$$

Geometric sum over  $F_0$  terms

$$C_L \sim \frac{1}{F_0^{-1} + \mathcal{M}}$$

Poles of  $C_L(E)$  are identified by  
 $\det [F_0^{-1}(E_n) + \mathcal{M}(E_n)] = 0$

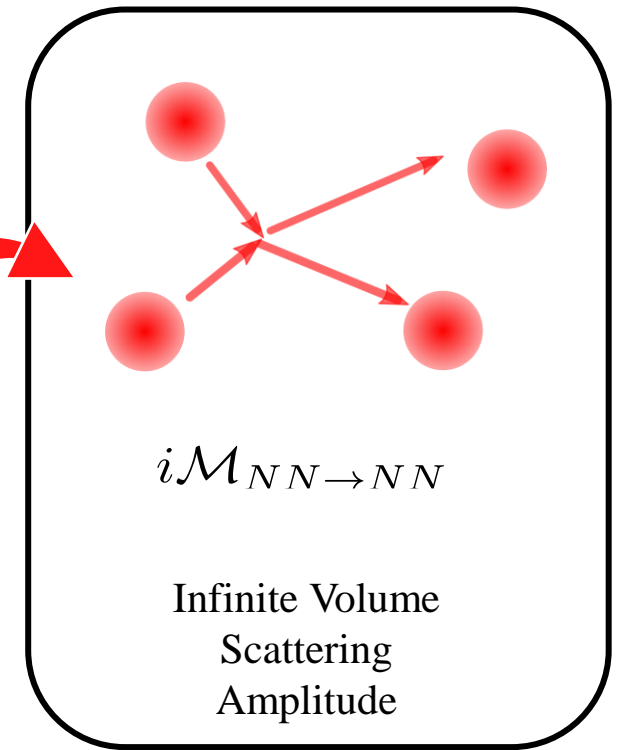
# Two Nucleon Scattering Amplitude



Lüscher's Quantization Condition

$$\det [F_0^{-1}(E_n) + \mathcal{M}(E_n)] = 0$$

Lüscher Commun. Math. Phys. 104, 177 (1986)  
Lüscher Commun. Math. Phys. 105, 153 (1986)  
Kim, Sachrajda, and Sharpe, Nucl. Phys. B727 (2005)



# FV Formalism

Review: Davoudi, Detmold, Shanahan, Orginos, Parreno, Savage, Wagman  
physrep.2020.10.004

Extended towards electro-weak current ( $\mathcal{J}$ ) interactions:

- Formalism for generalized  $0 + \mathcal{J} \rightarrow 2$  and  $1 + \mathcal{J} \rightarrow 2$  processes.

From LQCD:  $\gamma^* \rightarrow \pi\pi$  and  $\pi\gamma^* \rightarrow \pi\pi$  amplitudes.

- Formalism for  $2 + \mathcal{J} \rightarrow 2$  processes.

Value of  $L_{1,A}$  from LQCD via studying pp fusion  $pp \rightarrow de^+\nu$  process.

- Formalism for  $1 + 2\mathcal{J} \rightarrow 1$  processes.

$2\nu\beta\beta$  matrix elements (MEs) at  $m_\pi \sim 800$  MeV

- $K_L - K_S$  mass difference
- Formalism for  $1 + 2\mathcal{J} \rightarrow 1$  processes with massless leptonic propagators
- Formalism for  $2 + 2\mathcal{J} \rightarrow 2$  processes for  $2\nu\beta\beta$  and  $0\nu\beta\beta$ .
- Light sterile neutrino contribution to  $\pi^- \rightarrow \pi^+ e^- e^-$  from LQCD at the physical pion mass
- $\pi^- \rightarrow \pi^+ e^- e^-$  from LQCD at  $m_\pi$  in 300-430 MeV

Briceno, Hansen, and Walker-Loud (2015) Phys. Rev. D 91, 034501

Briceno and Hansen (2015), Phys. Rev. D 92 (7), 074509

Feng et al. (2015) Phys. Rev. D 91 (5), 054504

Briceno et al. (2015a) Phys. Rev. Lett. 115, 242001

Briceño and Davoudi (2013) Phys. Rev. D 88, 094507

Briceno and Hansen (2016) Phys. Rev. D 94 (1), 013008

NPLQCD Collaboration Phys. Rev. Lett. 119 (6) (2017) 62002.

Briceño, Davoudi, Hansen, Schindler and Baroni  
Phys. Rev. D 101, 014509

NPLQCD Collaboration Phys. Rev. D 96, 054505.

Christ, Izubuchi, Sachrajda, Soni, and Yu  
(RBC and UKQCD Collaborations)

Phys. Rev. D 88, 014508 (2013)

Christ, Feng, Jin, and Sachrajda Phys. Rev. D 103, 014507 (2021)

Feng, Jin, Wang, and Zhang Phys. Rev. D 103, 034508 (2021)

Davoudi and Kadam Phys. Rev. D 102, 114521 (2020)

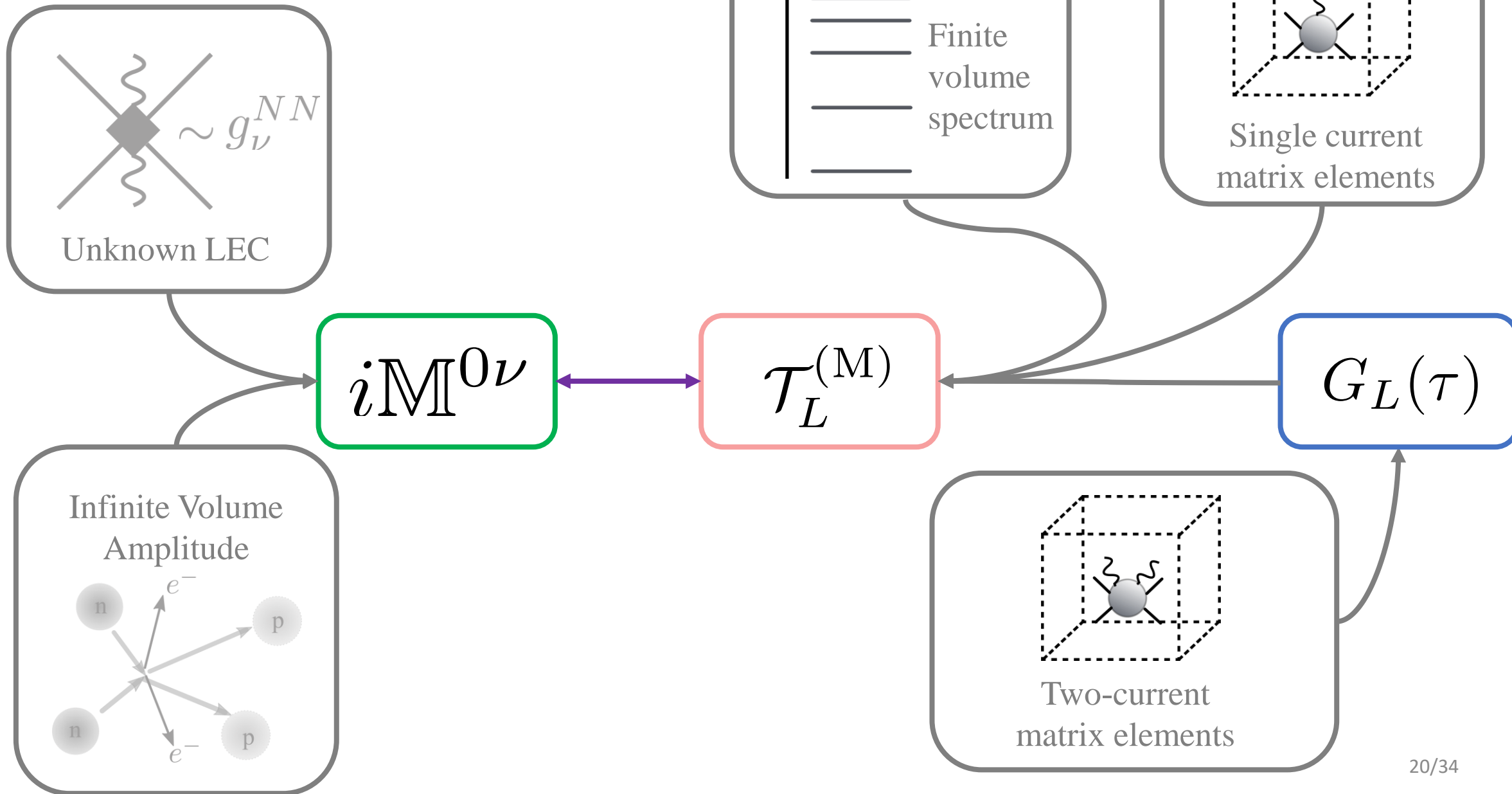
Davoudi and Kadam Phys. Rev. Lett. 126, 152003 (2021)

Tuo, Feng, and Jin arXiv:2206.00879

Detmold and Murphy arXiv:2004.07404

Detmold, Jay, Murphy, Oare, and Shanahan arXiv:2208.05322

# Constraining $g_\nu^{NN}$ from Lattice QCD



# $0\nu\beta\beta$ Decay

Finite Volume

For details see:

Davoudi and Kadam Phys. Rev. Lett. 126, 152003 (2021)

$$\mathcal{T}_L^{(M)} = \int_L d^3z \int dz_0 e^{iE_1 z_0} [\langle E_{n_f} | T^{(M)} [\mathcal{J}(z) S_\nu(z) \mathcal{J}(0)] | E_{n_i} \rangle ]_L$$

Evaluate the correlation function in EFT non-perturbatively

$$C_L^{0\nu} = \text{Diagram 1} + \text{Diagram 2}$$

Sum over quantized momenta

With neutrino propagator  $\sim \frac{1}{L^3} \sum_{\mathbf{q} \neq 0} \frac{m_{\beta\beta}}{|\mathbf{q}|^2}$

IR regulated by removing zero mode

# $0\nu\beta\beta$ Decay

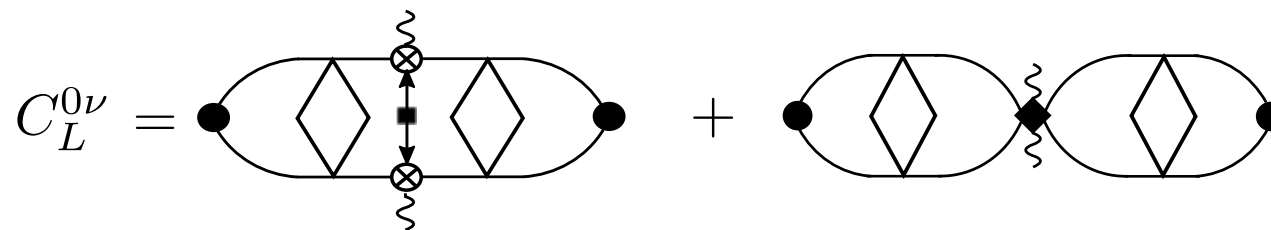
Finite Volume

For details see:

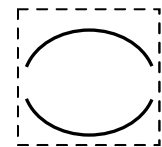
Davoudi and Kadam Phys. Rev. Lett. 126, 152003 (2021)

$$\mathcal{T}_L^{(M)} = \int_L d^3z \int dz_0 e^{iE_1 z_0} [\langle E_{n_f} | T^{(M)} [\mathcal{J}(z) S_\nu(z) \mathcal{J}(0)] | E_{n_i} \rangle ]_L$$

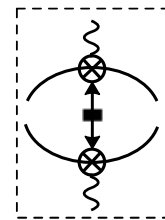
Evaluate the correlation function in EFT non-perturbatively



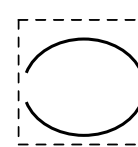
Identify and isolate FV corrections



$F_0(E_i)$

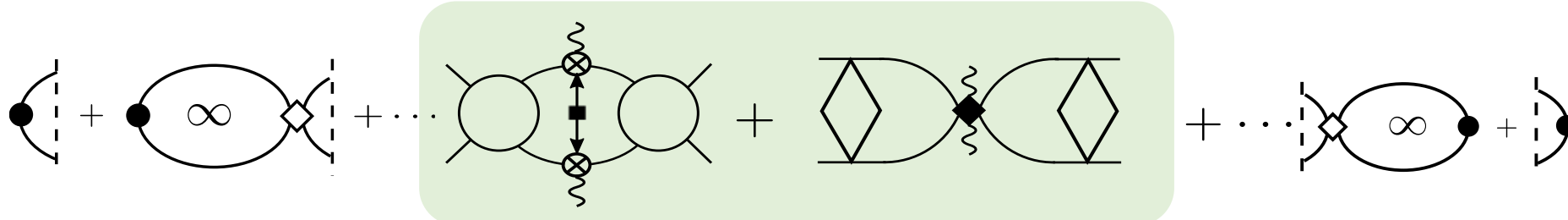


$\delta J^V$



$F_0(E_f)$

Rearrange to get infinite volume quantities



$iM^{0\nu}$

# Constraining $g_\nu^{NN}$ from Lattice QCD

For details see:

Davoudi and Kadam Phys. Rev. Lett. 126, 152003 (2021)

$$L^6 \left| \mathcal{T}_L^{(M)} \right|^2 = |\mathcal{R}^*(E_{n_f})| |iM^{0\nu}|^2 |\mathcal{R}^*(E_{n_i})|$$

Lellouch Luscher  
residue matrix

$$\mathcal{R}(E_n) = \lim_{E \rightarrow E_n} \frac{(E - E_n)}{F_0^{-1} + \mathcal{M}}$$

# Constraining $g_V^{NN}$ from Lattice QCD

For details see:

Davoudi and Kadam Phys. Rev. Lett. 126, 152003 (2021)

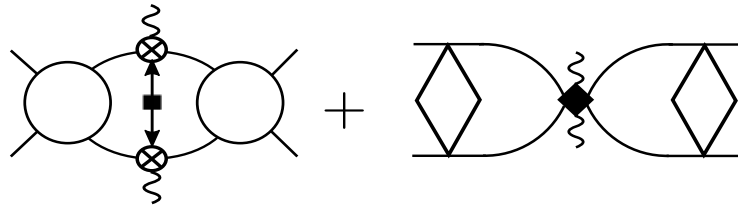
$$L^6 \left| \mathcal{T}_L^{(M)} \right|^2 = \left| \mathcal{R}^*(E_{n_f}) \right| \left| i\mathbb{M}^{0\nu} \right|^2 \left| \mathcal{R}^*(E_{n_i}) \right|$$

Lellouch Luscher  
residue matrix

$$\mathcal{R}(E_n) = \lim_{E \rightarrow E_n} \frac{(E - E_n)}{F_0^{-1} + \mathcal{M}}$$

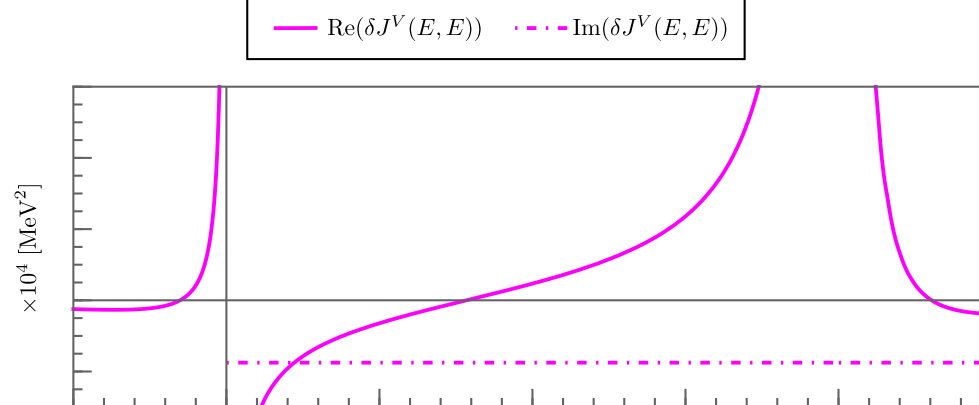
$$i\mathbb{M}^{0\nu} = i\mathcal{M}_{nn \rightarrow pp}^{(\text{Int.})} - m_{\beta\beta} (1 + 3g_A^2) \mathcal{M}_{nn} \delta J^V \mathcal{M}_{pp}$$

$$i\mathcal{M}_{nn \rightarrow pp}^{(\text{Int.})} =$$



Physical LO two-nucleon amplitude

$$\text{Diagram} = \text{Diagram} \sim C_0 + \text{Diagram} + \dots$$

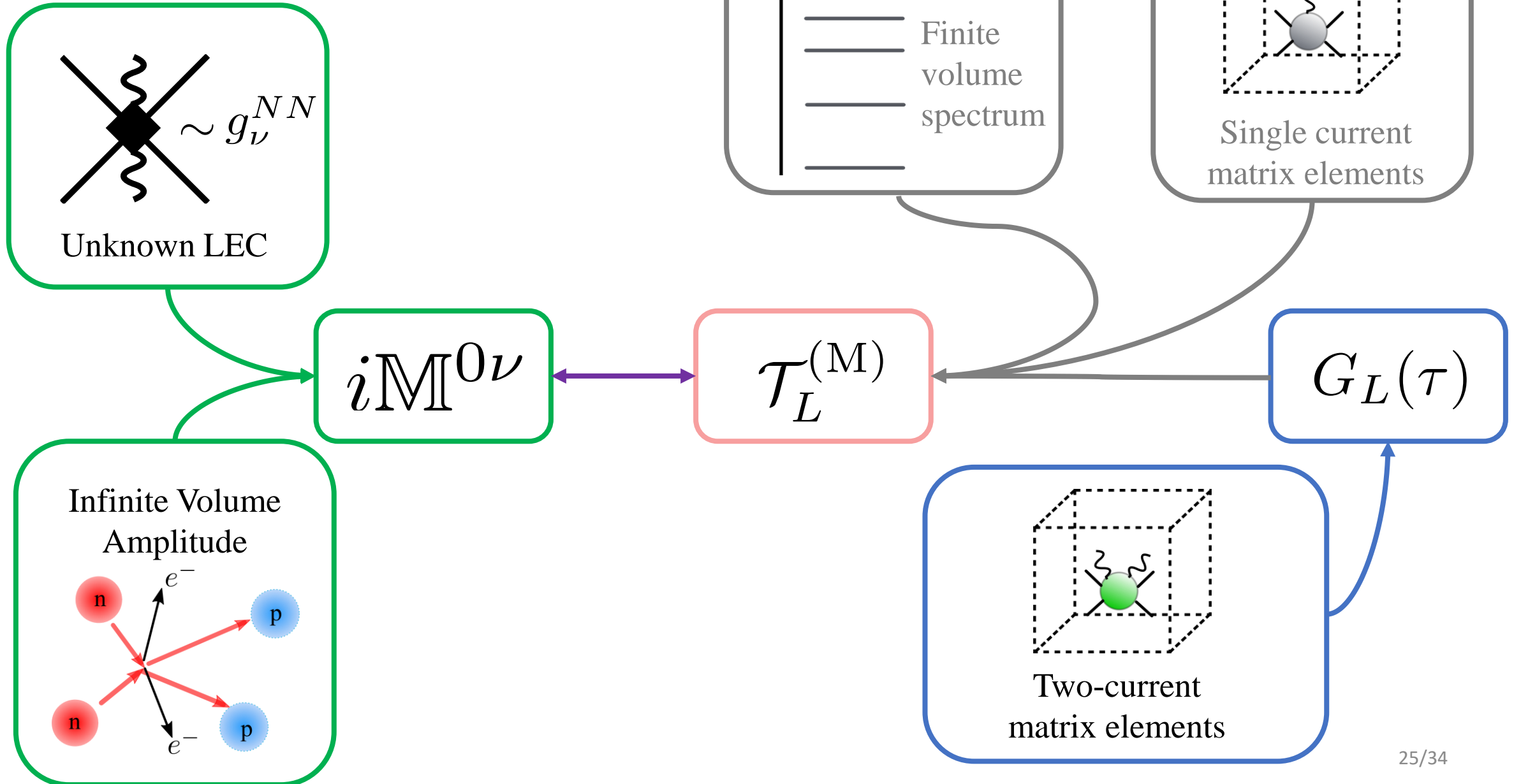


Finite volume corrections

$$\text{Diagram} \quad \sum_{\vec{k}} = \int_{\vec{k}} + \delta J^V$$



# Constraining $g_\nu^{NN}$ from LQCD



$$\mathcal{T}_L^{(M)}$$

Minkowski Signature  
Correlation Function

$$\mathcal{T}_L^{(M)} = \int_L d^3 z \int dz_0 e^{iEz_0} [\langle E_{n_f} | T^{(M)} [\mathcal{J}(z) S_\nu(z) \mathcal{J}(0)] | E_{n_i} \rangle]_L$$

?

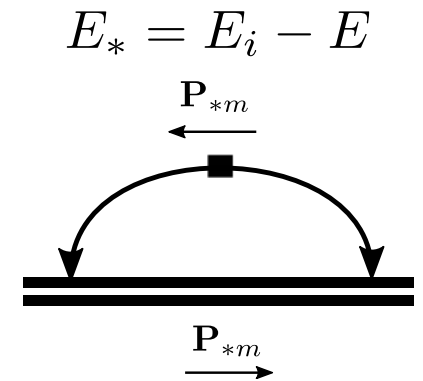
$$G_L(\tau)$$

Euclidean Time  
Four-point Correlation  
Function from LQCD

$$G_L(\tau) = \int_L d^3 z [\langle E_f, L | T^{(E)} [\mathcal{J}^{(E)}(\tau, z) S_\nu^E(\tau, z) \mathcal{J}^{(E)}(0)] | E_i, L \rangle]_L,$$

Plugging back the missing time integral

$$\mathcal{T}_L^{(E)} \stackrel{?}{=} \int d\tau e^{E\tau} G_L(\tau) \quad \sim \int_0^\infty d\tau e^{-(|\mathbf{P}_{*m}| + E_{*m} - E_*)\tau}$$



$$\mathcal{T}_L^{(M)}$$

Minkowski Signature  
Correlation Function

$$\mathcal{T}_L^{(M)} = \int_L d^3z \int dz_0 e^{iEz_0} [\langle E_{n_f} | T^{(M)}[\mathcal{J}(z) S_\nu(z) \mathcal{J}(0)] | E_{n_i} \rangle]_L$$

?

$$G_L(\tau)$$

Euclidean Time  
Four-point Correlation  
Function from LQCD

$$G_L(\tau) = \int_L d^3z [\langle E_f, L | T^{(E)}[\mathcal{J}^{(E)}(\tau, z) S_\nu^E(\tau, z) \mathcal{J}^{(E)}(0)] | E_i, L \rangle]_L,$$

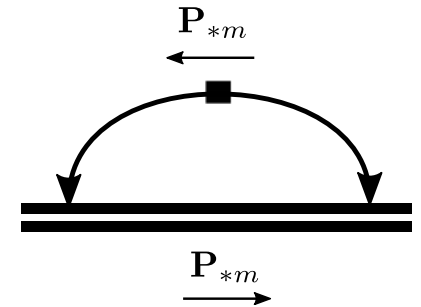
Plugging back the missing time integral

$$\mathcal{T}_L^{(E)} \stackrel{?}{=} \int d\tau e^{E\tau} G_L(\tau) \sim \int_0^\infty d\tau e^{-(|\mathbf{P}_{*m}| + E_{*m} - E_*)\tau}$$

Diverges for  $|\mathbf{P}_{*m}| + E_{*m} < E_*$

$$E_* = E_i - E$$

Diverges for intermediate states that can go on-shell



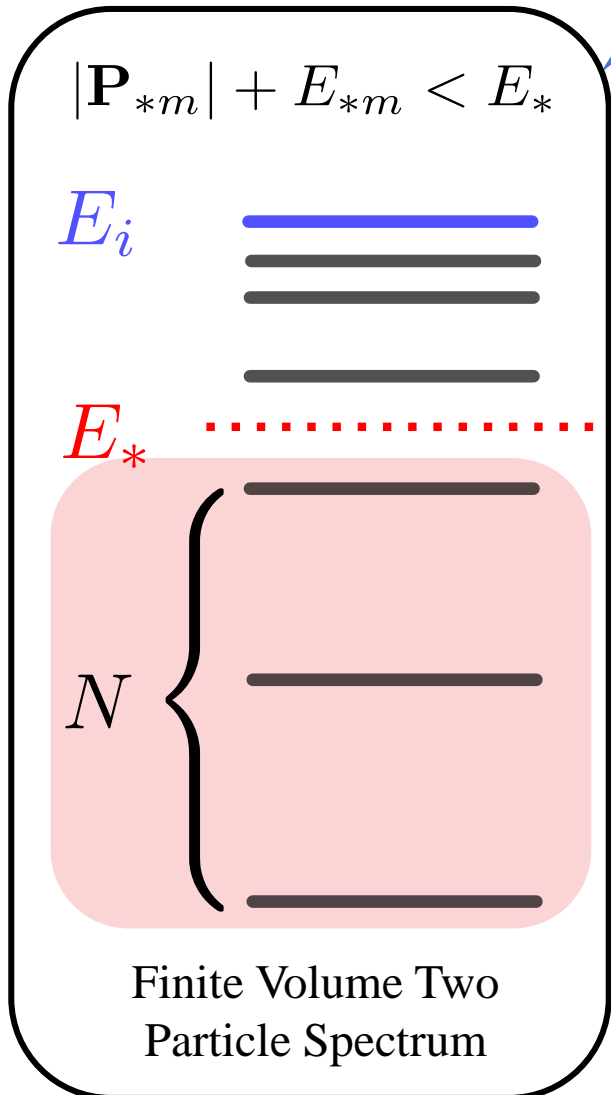
Need to remove these divergences for analytic continuation!!

Where is the divergence coming from?  
Two particle FV states which can go on-shell

Constructing divergent contributions

Spectral representation by integrating over time

$$\mathcal{T}_L^{(M)} = i \sum_{m=0}^{\infty} \frac{c_m}{E_* - E_{*m} - |\mathbf{P}_{*m}| + i\epsilon}$$



Two-body spectrum to identify  $N$  low-lying states

$c_m \sim$  Finite volume matrix elements of single hadronic current between the initial (final) and intermediate states

$$G_L^<(\tau) \equiv \sum_{m=0}^{N-1} c_m \theta(\tau) e^{-(|\mathbf{P}_{*m}| + E_{*m} - E_f)|\tau|}$$

Can be analytically continued to Minkowski space

$G_L(\tau)$   
Four-point Function From LQCD

$$\mathcal{T}_L^{(E) \geq} \equiv \int d\tau e^{E\tau} [G_L(\tau) - G_L^<(\tau)]$$

# What do we want?

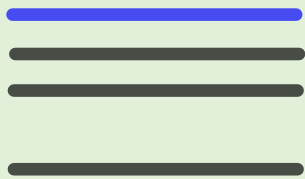
$$\mathcal{T}_L^{(M)} = i \sum_{m=0}^{\infty} \frac{c_m}{E_* - E_{*m} - |\mathbf{P}_{*m}| + i\epsilon}$$

So far, we have

$$\mathcal{T}_L^{(E)} \geq \equiv \int d\tau e^{E\tau} [G_L(\tau) - G_L^<(\tau)]$$

$$|\mathbf{P}_{*m}| + E_{*m} < E_*$$

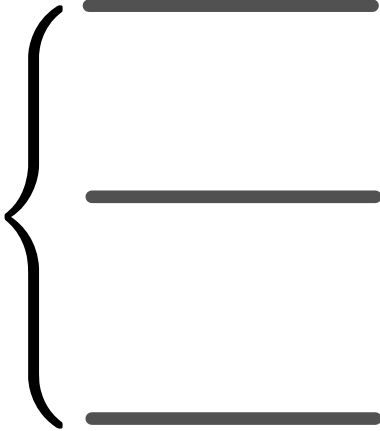
$E_i$



$E_*$



$N$



Finite Volume Two  
Particle Spectrum

# What do we want?

$$\mathcal{T}_L^{(M)} = i \sum_{m=0}^{\infty} \frac{c_m}{E_* - E_{*m} - |\mathbf{P}_{*m}| + i\epsilon}$$

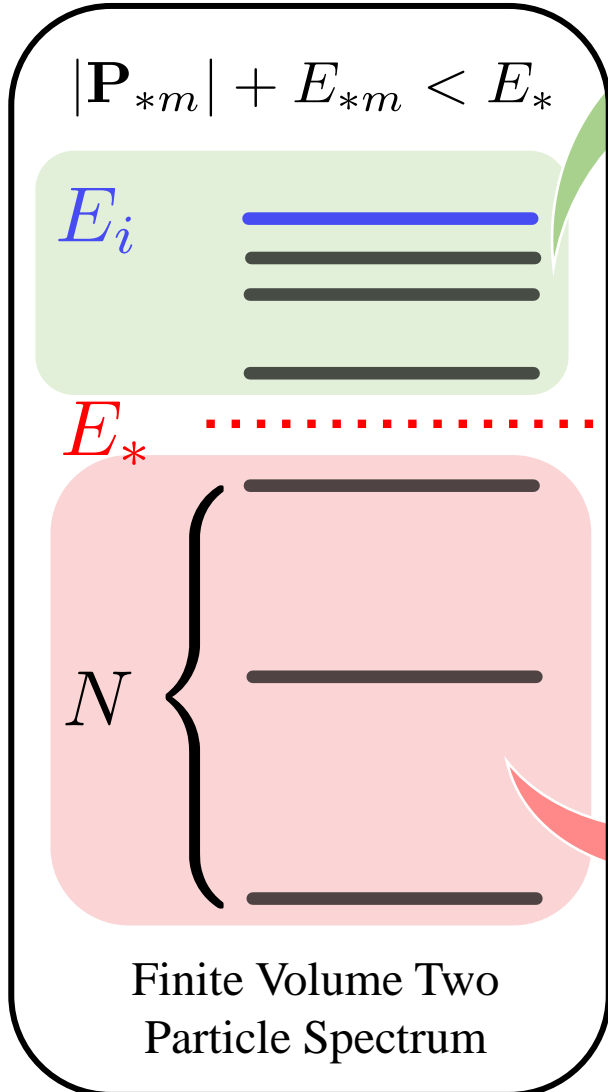
So far, we have

$$\mathcal{T}_L^{(E) \geq} \equiv \int d\tau e^{E\tau} [G_L(\tau) - G_L^<(\tau)]$$

Missing Piece

$$\mathcal{T}_L^{(E) <} \equiv \sum_{m=0}^{N-1} \frac{c_m}{E_* - E_{*m} - |\mathbf{P}_{*m}|}$$

$$\mathcal{T}_L^{(M)} = i\mathcal{T}_L^{(E) <} + i\mathcal{T}_L^{(E) \geq}$$



# What do we want?

$$\mathcal{T}_L^{(M)} = i \sum_{m=0}^{\infty} \frac{c_m}{E_* - E_{*m} - |\mathbf{P}_{*m}| + i\epsilon}$$

For  $L = 8$  fm

$$E_{1S_0} = -2.728, 19.043, \dots \text{ MeV}$$

$$E_{*m} = -5.579, 13.688, \dots \text{ MeV}$$

$$|\mathbf{P}_*| = 2\pi/L \approx 155 \text{ MeV}$$

$$i\mathcal{T}_L^{(E)} = i \int d\tau e^{E_1\tau} G_L^{(E)}(\tau)$$

So far, we have

$$\mathcal{T}_L^{(E) \geq} \equiv \int d\tau e^{E\tau} [G_L(\tau) - G_L^<(\tau)]$$

Missing Piece

$$\mathcal{T}_L^{(E) <} \equiv \sum_{m=0}^{N-1} \frac{c_m}{E_* - E_{*m} - |\mathbf{P}_{*m}|}$$

$$\mathcal{T}_L^{(M)} = i\mathcal{T}_L^{(E) <} + i\mathcal{T}_L^{(E) \geq}$$

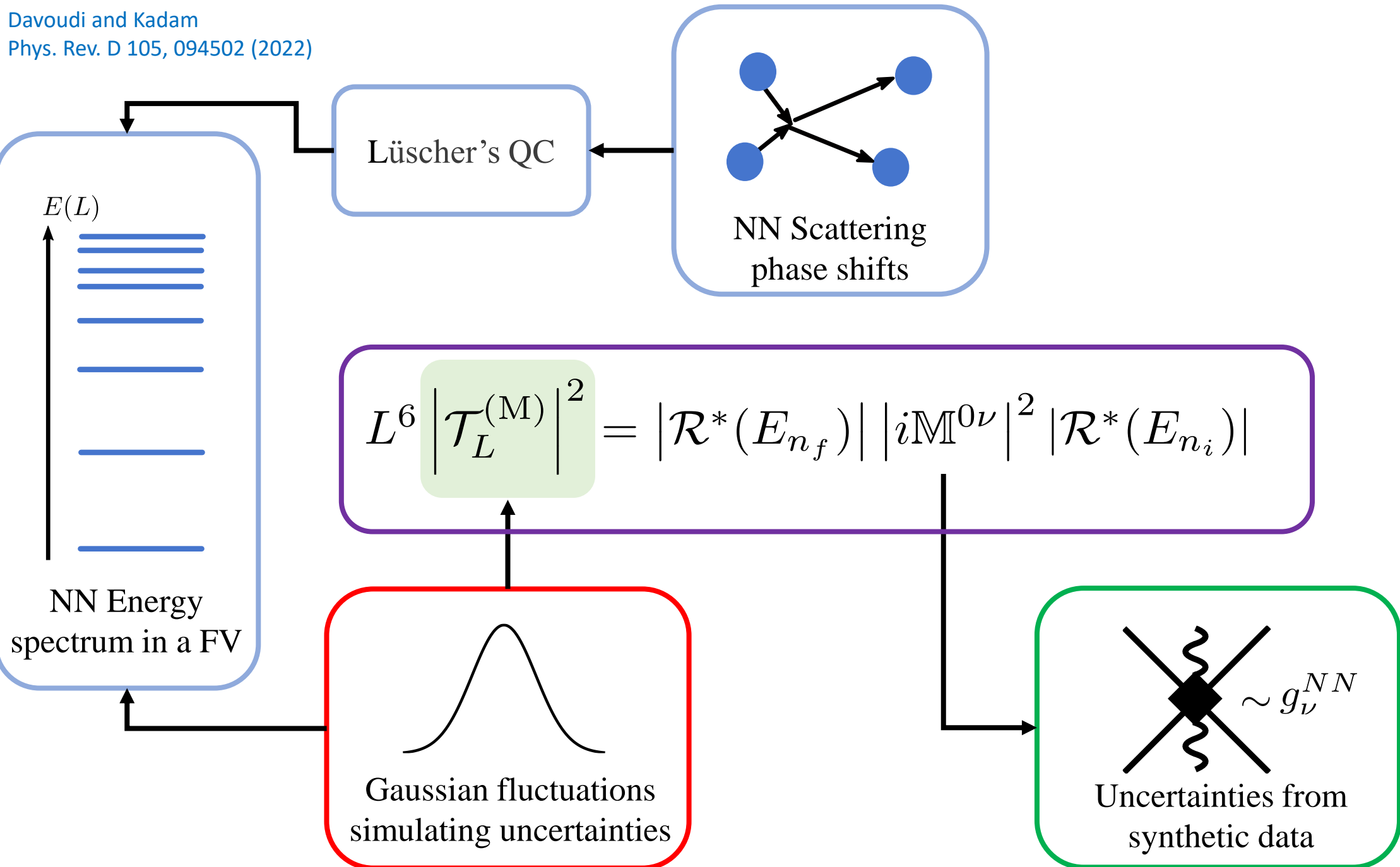
$$|\mathbf{P}_{*m}| + E_{*m} < E_*$$

$E_i$

$E_*$

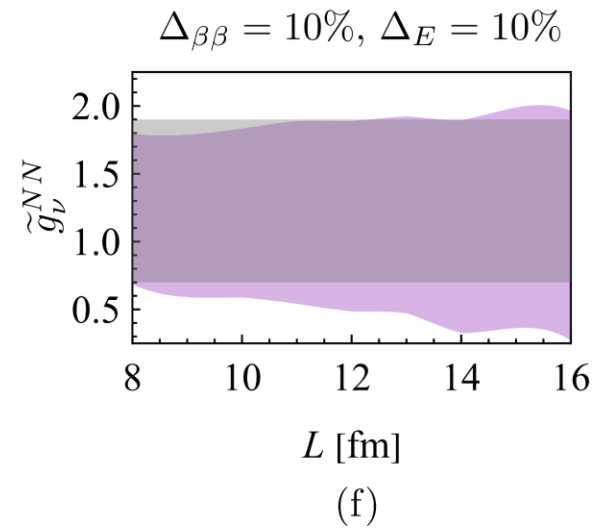
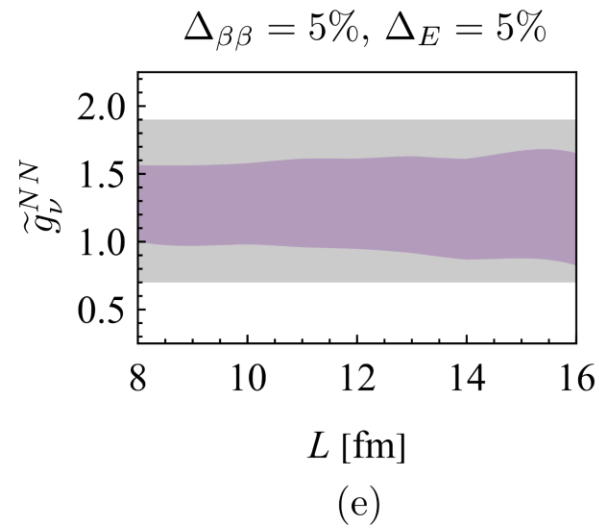
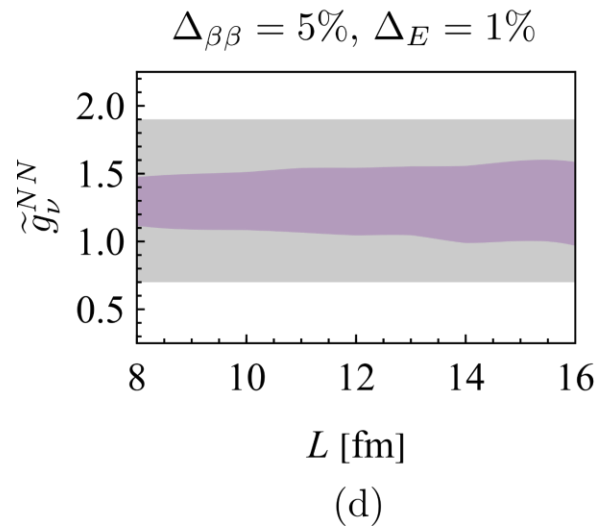
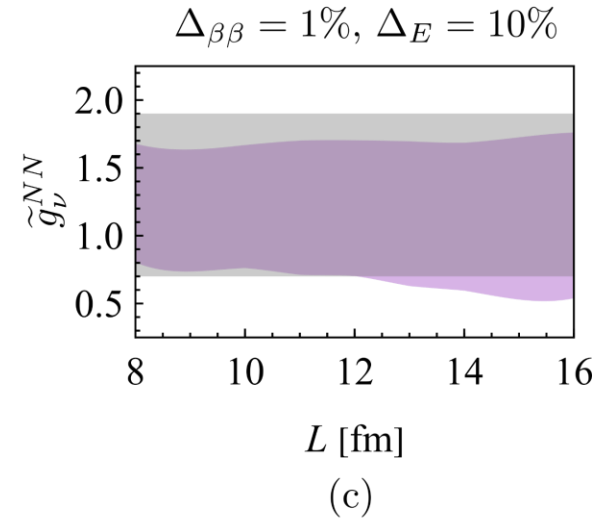
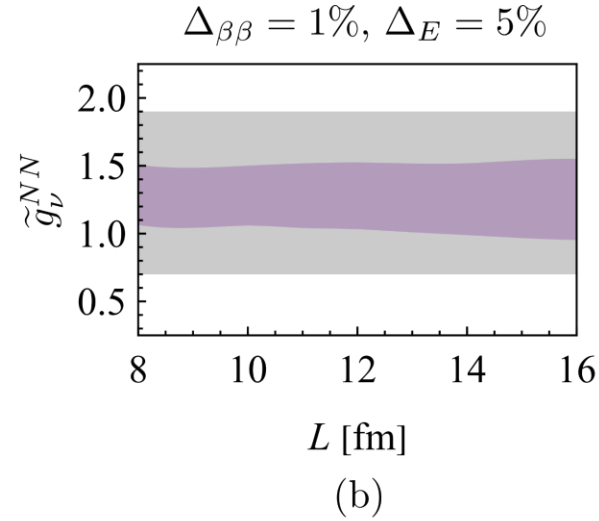
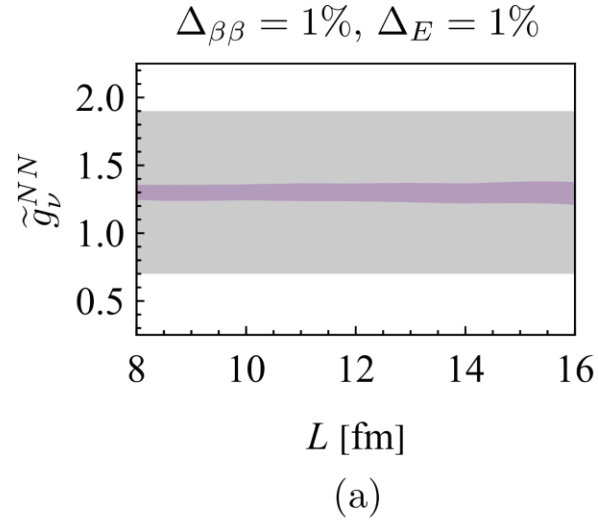
$N$

Finite Volume Two  
Particle Spectrum

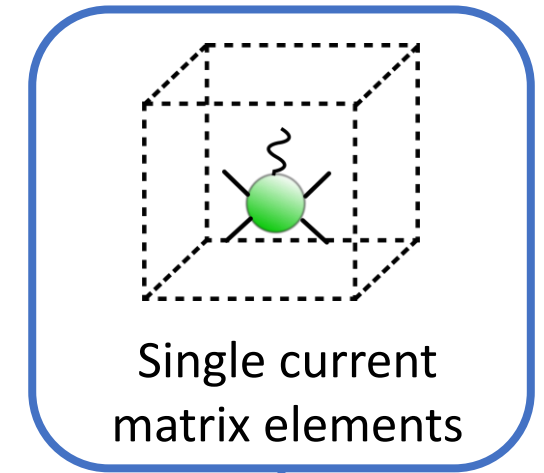
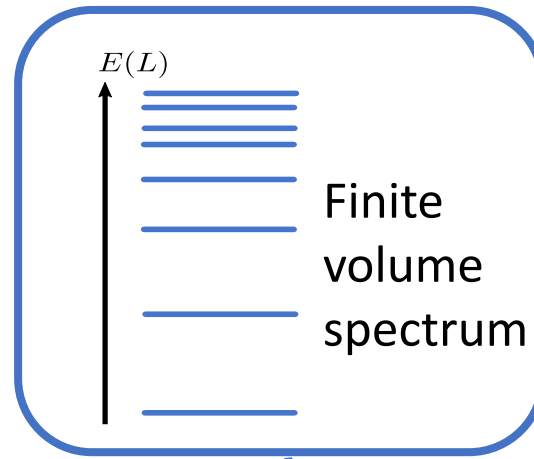
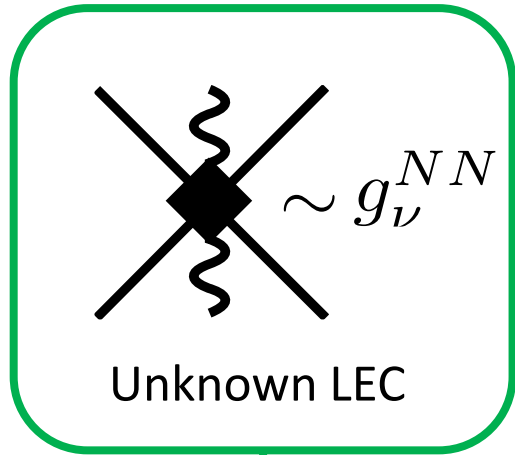




$\Delta_{\beta\beta}$  : Uncertainty in four-point function  
 $\Delta_E$  : Uncertainty in NN energy eigenvalues



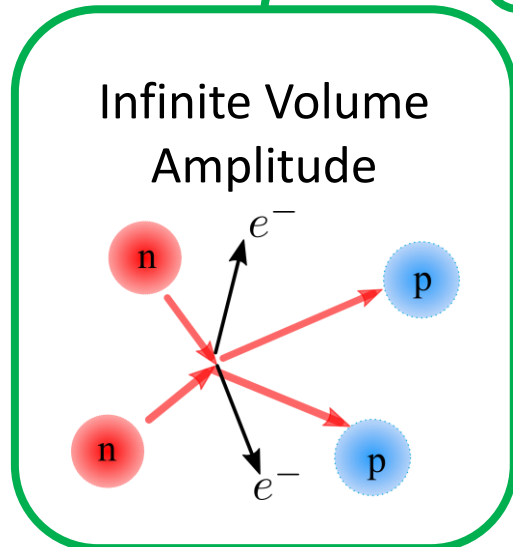
# Summary



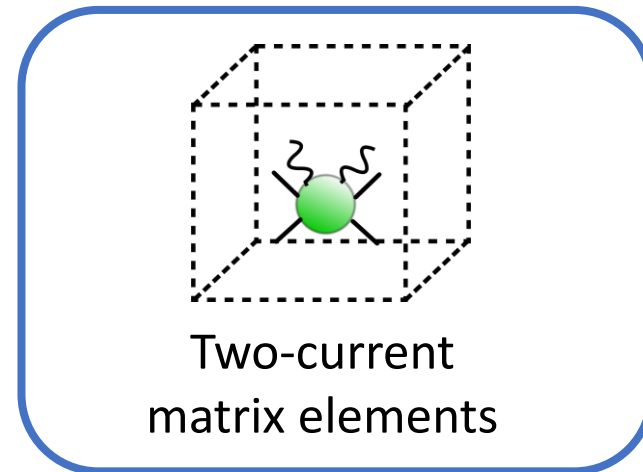
$$iM^{0\nu}$$

$$\mathcal{T}_L^{(M)}$$

$$G_L(\tau)$$



Thank You !



# Backup

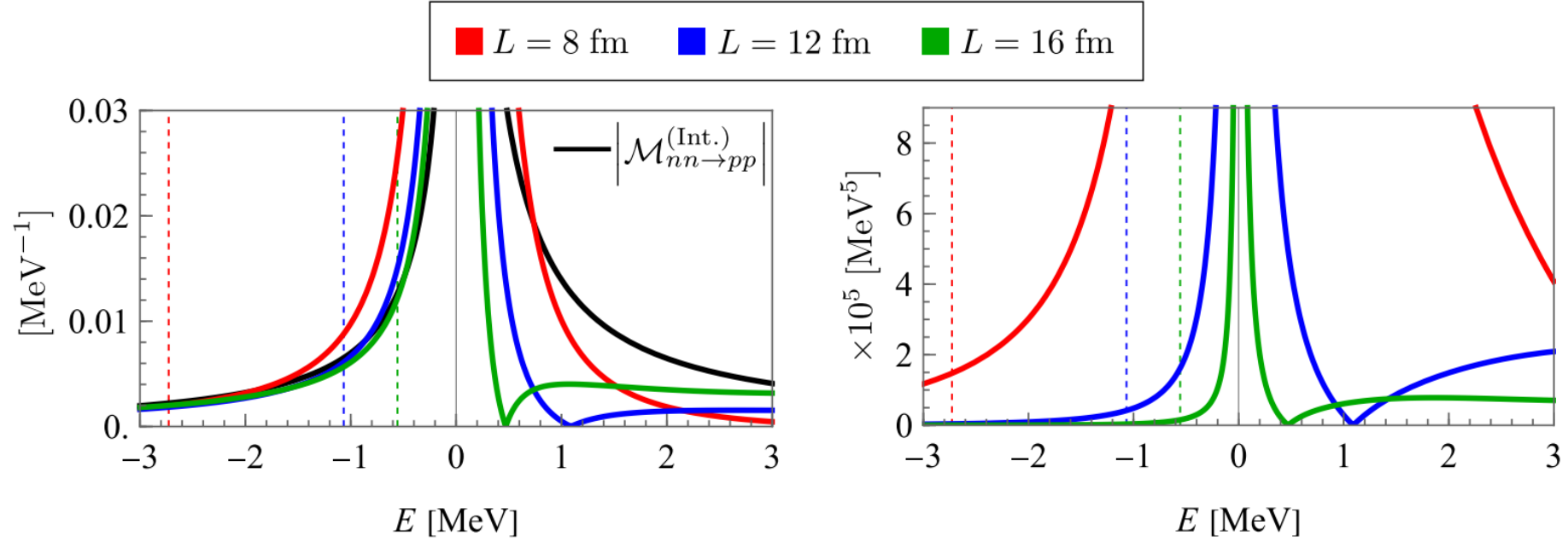


FIG. 7.  $|\mathcal{M}_{nn \rightarrow pp}^{0\nu, V(\text{Int.})}|$  (left) and  $|\mathcal{T}_L^{(M)}|$  (right) functions defined in Eqs. (30)-(28), with  $L = 8$  fm (red),  $L = 12$  fm (blue), and  $L = 16$  fm (green) are plotted against the CM energy of the NN state, considering the kinematics  $E_i = E_f \equiv E$ . The effective neutrino mass  $m_{\beta\beta}$  is set to 1 MeV. The dashed lines in both panels denote the ground-state energy eigenvalues in the corresponding volumes obtained from the quantization condition in Eq. (9) (as plotted in Fig. 2). Selected numerical values for the functions shown are provided in Appendix A.

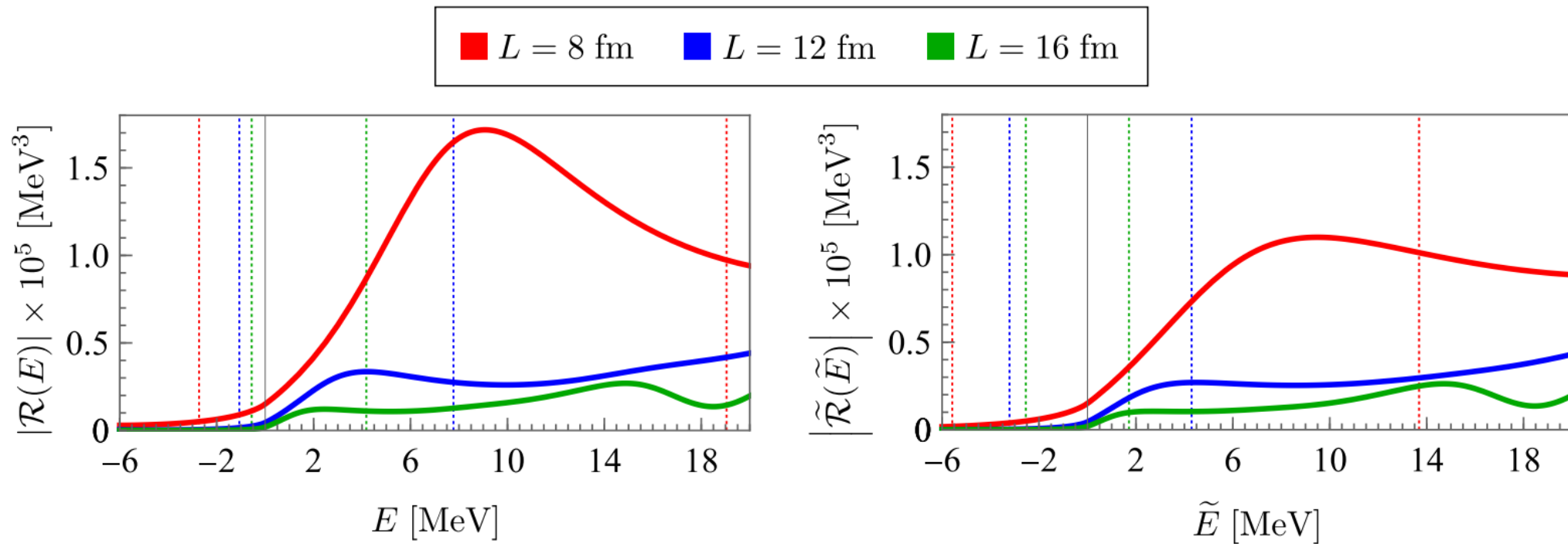


FIG. 3. The absolute values of the LL residue function in the  $^1S_0$  (left) and  $^3S_1$  (right) channels is plotted against the CM energy for three different volumes with  $L = 8$  fm (red),  $L = 12$  fm (blue), and  $L = 16$  fm (green). Dashed lines indicate energy eigenvalues in the respective volumes. The numerical values of  $|\mathcal{R}|$  and  $|\tilde{\mathcal{R}}|$  evaluated at the FV ground- and first excited-state energies in the corresponding volumes are provided in Appendix A.

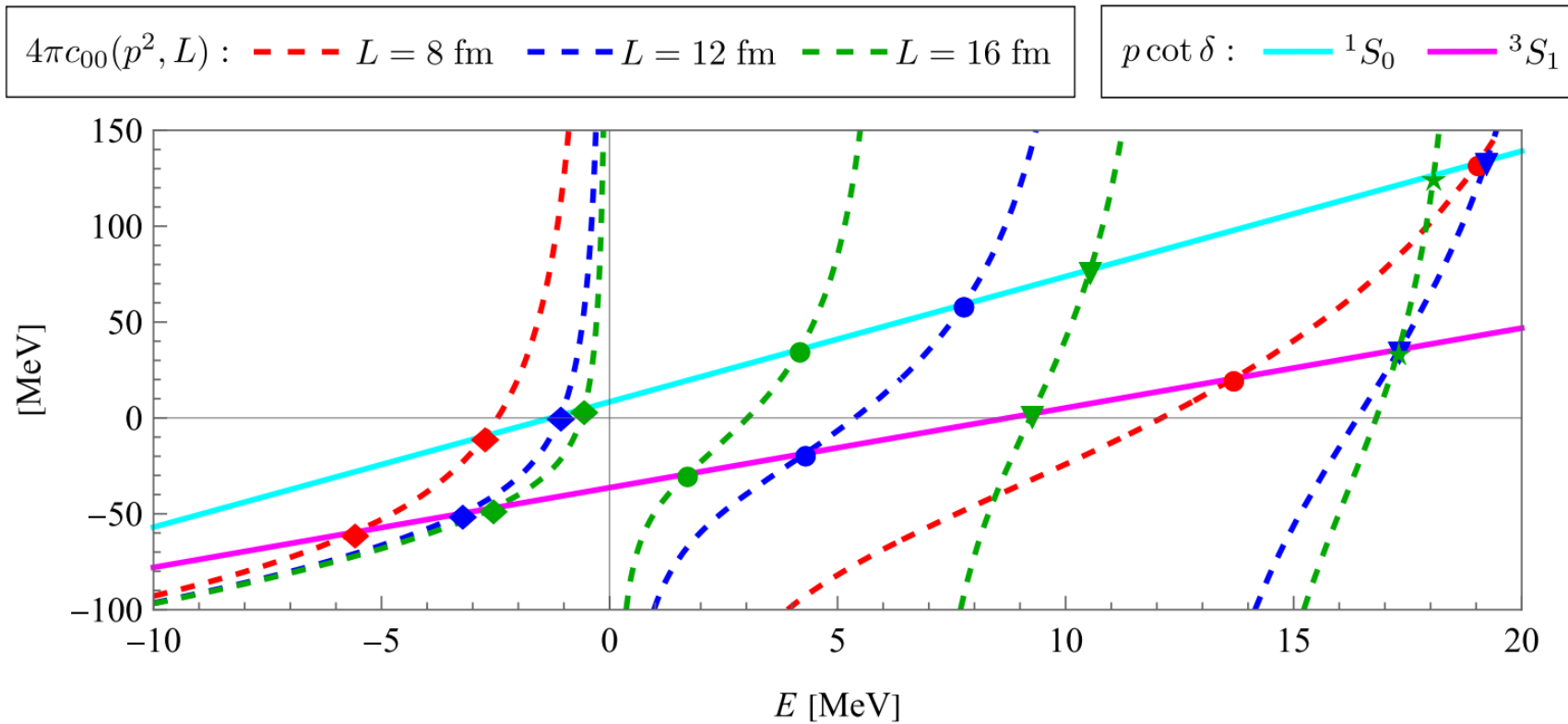


FIG. 2. The effective-range function (solid lines) and Lüscher's function (dotted lines) in Eq. (9) are plotted independently against the CM energy of NN systems. Equation (4) is used for the effective-range function with the effective-range expansion parameters given in Eq. (14) for the two channels,  $^1S_0$  (cyan) and  $^3S_1$  (magenta). The function  $4\pi c_{00}(p^2, L)$  is plotted for three different volumes with  $L = 8$  fm (red),  $L = 12$  fm (blue) and  $L = 16$  fm (green). The diamonds, circles, triangles, and stars denote, respectively, the location of energy eigenvalues of the ground, first, second, and third excited states in each volume, and satisfy the quantization condition in Eq. (9) (and its counterpart for the  $^3S_1$  channel). The numerical values associated with this figure are provided in Appendix A.

# $0\nu\beta\beta$ Decay

*Infinite Volume*

At LO in Pionless EFT

Cirigliano, Dekens, de Vries,  
Graesser, Mereghetti, Pastore,  
Piarulli, Van Kolck and Wiringa  
Phys. Rev. C 100, 055504 (2019)

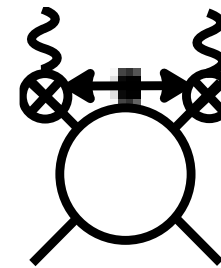
Cirigliano, Dekens, de Vries,  
Graesses, Mereghetti,  
Pastore and van Klock  
Phys. Rev. Lett. 120, 202001

$$i\mathcal{M}_{0\nu} =$$

The diagram shows five Feynman diagrams representing the leading order (LO) contribution to the  $0\nu\beta\beta$  decay amplitude. The first diagram is a tree-level exchange of a neutrino between two nucleons, with a square representing the potential and a wavy line representing a photon. The second and third diagrams are loop diagrams with a photon and a neutrino. The fourth and fifth diagrams are also loop diagrams with a photon and a neutrino.

$$\sim \frac{m_{\beta\beta}}{|\mathbf{q}|^2}$$

Static Neutrino Potential



Radiative Neutrinos  
Higher Order

# $0\nu\beta\beta$ Decay

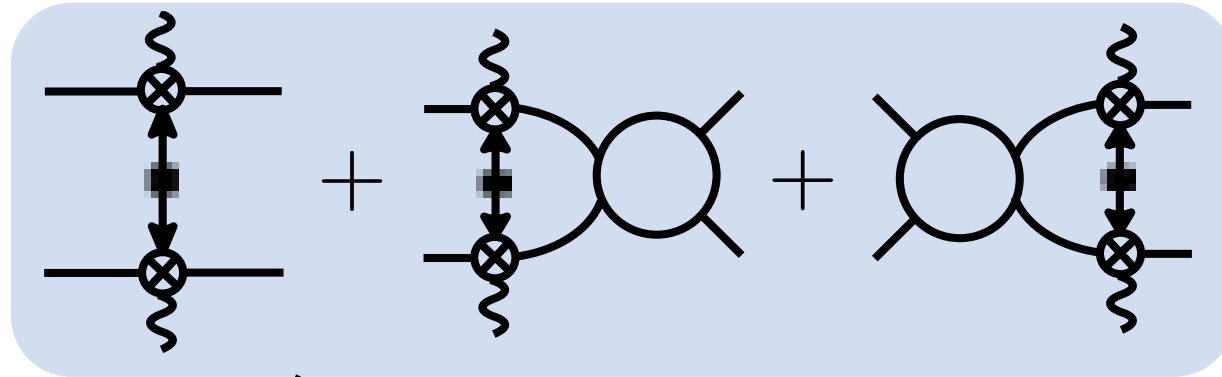
Infinite Volume

At LO in Pionless EFT

Cirigliano, Dekens, de Vries,  
Gaesser, Mereghetti, Pastore,  
Piarulli, Van Kolck and Wiringa  
Phys. Rev. C 100, 055504 (2019)

Cirigliano, Dekens, de Vries,  
Gaesses, Mereghetti,  
Pastore and van Klock  
Phys. Rev. Lett. 120, 202001

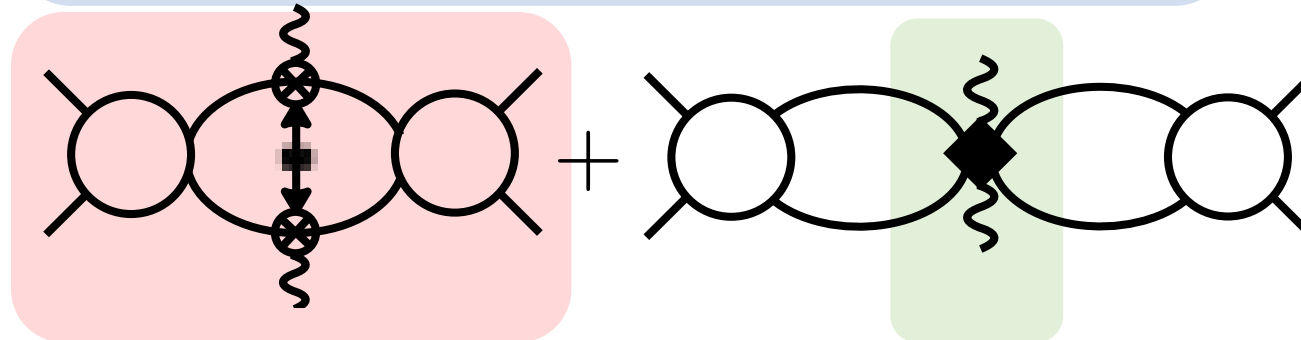
$$i\mathcal{M}_{0\nu} =$$



Won't contribute to FV correlation function

Divergent

+



Scale dependent LEC

$$I_{0\nu}^\infty(E_i, E_f) \sim \text{Diagram} \xrightarrow{\text{New LEC}} \text{Diagram} \sim g_\nu^{NN}$$

$$\mu \frac{d}{d\mu} \left( \frac{g_\nu^{NN}}{C_0^2} \right) = \frac{1+3g_A^2}{2} \frac{M_N^2}{16\pi^2}$$



TABLE I. Lower bounds achievable for  $m_{\beta\beta}$  by some  $0\nu\beta\beta$  experiments, depending on their reached sensitivities (upper group) or sensitivity goals (lower group). The different results correspond to the different quenching of  $g_A$ , according to the definitions in Eq. (9). The  $1\sigma$  uncertainties on  $m_{\beta\beta}$  are calculated by assuming uncertainties both on the matrix elements and phase space factors, according to [1] and [8], respectively.

Experiment	Isotope	$t^{1/2}(90\% \text{ C.L.})(10^{25} \text{ yr})$	Lower bound for $m_{\beta\beta}(\text{eV})$		
			$g_{\text{nucleon}}$	$g_{\text{quark}}$	$g_{\text{phen.}}$
IGEX [9]	$^{76}\text{Ge}$	1.57	$0.31 \pm 0.03$	$0.49 \pm 0.05$	$1.44 \pm 0.16$
HEIDELBERG-MOSCOW [10]	$^{76}\text{Ge}$	1.9	$0.28 \pm 0.03$	$0.44 \pm 0.05$	$1.31 \pm 0.14$
GERDA-I [11]	$^{76}\text{Ge}$	2.1	$0.26 \pm 0.03$	$0.42 \pm 0.05$	$1.25 \pm 0.14$
KamLAND-Zen-I [12]	$^{136}\text{Xe}$	1.9	$0.18 \pm 0.02$	$0.29 \pm 0.03$	$1.06 \pm 0.12$
KamLAND-Zen-II [13]	$^{136}\text{Xe}$	1.3	$0.22 \pm 0.02$	$0.35 \pm 0.04$	$1.28 \pm 0.14$
EXO-200 [14]	$^{136}\text{Xe}$	1.1	$0.24 \pm 0.03$	$0.38 \pm 0.04$	$1.39 \pm 0.15$
Combined Ge [11]	$^{76}\text{Ge}$	3.0	$0.22 \pm 0.02$	$0.35 \pm 0.04$	$1.05 \pm 0.11$
Combined Xe	$^{136}\text{Xe}$	2.6	$0.15 \pm 0.02$	$0.25 \pm 0.03$	$0.91 \pm 0.10$
Combined Ge + Xe	$^{76}\text{Ge}/^{136}\text{Xe}$		$0.15 \pm 0.01$	$0.24 \pm 0.02$	$0.81 \pm 0.07$
CUORE [15]	$^{130}\text{Te}$	9.5	$0.07 \pm 0.01$	$0.11 \pm 0.01$	$0.39 \pm 0.04$
GERDA-II [16]	$^{76}\text{Ge}$	15	$0.10 \pm 0.01$	$0.16 \pm 0.02$	$0.47 \pm 0.05$
SuperNEMO [17]	$^{82}\text{Se}$	10	$0.07 \pm 0.01$	$0.12 \pm 0.01$	$0.36 \pm 0.04$

TABLE II. Sensitivity and exposure necessary to discriminate between  $\mathcal{NH}$  and  $\mathcal{IH}$ : the goal is  $m_{\beta\beta} = 8 \text{ meV}$ . The two cases refer to the unquenched value of  $g_A = g_{\text{nucleon}}$  (mega) and  $g_A = g_{\text{phen.}}$  (ultimate). The calculations are performed assuming *zero background* experiments with 100% detection efficiency and no fiducial volume cuts. The last column shows the maximum value of the product  $B \cdot \Delta$  in order to actually comply with the zero background condition.

Experiment	Isotope	$t^{1/2}(\text{yr})$	Exposure (estimate)	
			$M \cdot T \text{ (ton} \cdot \text{yr)}$	$B \cdot \Delta_{(\text{zero bkg})} \text{ (counts/kg/yr)}$
Mega Te	$^{130}\text{Te}$	$6.8 \times 10^{27}$	2.1	$4.7 \times 10^{-4}$
Mega Ge	$^{76}\text{Ge}$	$2.3 \times 10^{28}$	4.1	$2.4 \times 10^{-4}$
Mega Xe	$^{136}\text{Xe}$	$9.7 \times 10^{27}$	3.2	$3.2 \times 10^{-4}$
Ultimate Te	$^{130}\text{Te}$	$2.3 \times 10^{29}$	71	$1.4 \times 10^{-5}$
Ultimate Ge	$^{76}\text{Ge}$	$5.1 \times 10^{29}$	93	$1.1 \times 10^{-5}$
Ultimate Xe	$^{136}\text{Xe}$	$3.3 \times 10^{29}$	109	$9.2 \times 10^{-6}$

**Table 1.** Limits on neutrinoless DBDs  $T_{1/2}^{0\nu\text{-exp}}$  (claim for evidence is denoted in [42]).  $Q_{\beta\beta}$ :  $Q$ -value for the  $0^+ \rightarrow 0^+$  ground-state transition.  $G^{0\nu}$ : kinematical (phase space volume) factor ( $g_A = 1.25$  and  $R = 1.2 \text{ fm } A^{1/3}$ ).  $\langle m_\nu \rangle$ : the upper limit on the effective Majorana neutrino mass, deduced from  $T_{1/2}^{0\nu\text{-exp}}$  by assuming the ISM [236] ( $g_A^{\text{eff}} = 1.25$ , UCOM src), the EDF [131] ( $g_A^{\text{eff}} = 1.25$ , UCOM src), the (R)QRPA ( $1.00 \leq g_A^{\text{eff}} \leq 1.25$ , the modern self-consistent treatment of src), and the IBM-2 [130] ( $1.00 \leq g_A^{\text{eff}} \leq 1.25$ , Miller–Spencer src), **NMEs** (see section 10). src means short-range correlations.

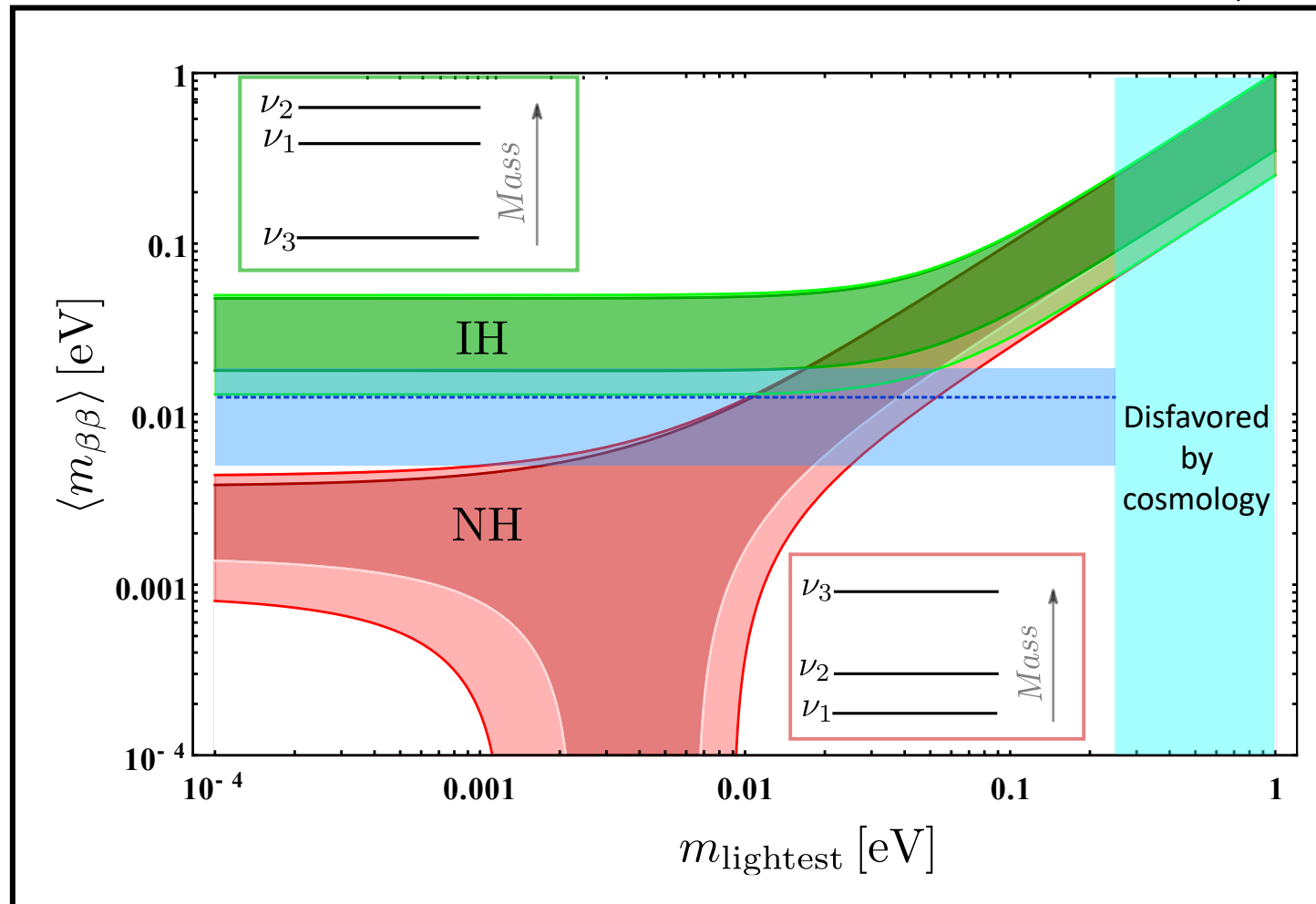
Isotope	$A$ (%)	$Q_{\beta\beta}$ (MeV)	$G^{0\nu}$ ( $10^{-14}$ y)	$T_{1/2}^{0\nu\text{-exp}}$ ( $10^{24}$ y)	NME	$ \langle m_\nu \rangle $ eV (eV)	Future experiments
$^{48}\text{Ca}$	0.19	4.276	7.15	0.014 [237]	ISM EDF	19.1 7.0	CANDLES
$^{76}\text{Ge}$	7.8	2.039	0.71	19 [36, 227, 228]	ISM, EDF (R)QRPA EDF	0.51, 0.31 (0.20, 0.32) (0.26, 0.35)	GERDA
	7.8	2.039	0.71	22 [42]	ISM, EDF (R)QRPA EDF	0.47, 0.29 (0.18, 0.30) (0.24, 0.32)	—
	7.8	2.039	0.71	16 [229, 230]	ISM, EDF (R)QRPA EDF	0.55, 0.34 (0.22, 0.35) (0.28, 0.38)	MAJORANA
$^{82}\text{Se}$	9.2	2.992	3.11	0.36 [38, 234, 235]	ISM, EDF (R)QRPA EDF	1.88, 1.17 (0.76, 1.28) (1.12, 1.49)	SuperNEMO MOON
$^{100}\text{Mo}$	9.6	3.034	5.03	1.0 [38, 234]	EDF	0.46	MOON
					(R)QRPA EDF	(0.38, 0.73) (0.62, 1.06)	AMoRE
$^{116}\text{Cd}$	7.5	2.804	5.44	0.17 [238]	EDF	1.15	COBRA
					(R)QRPA	(1.20, 2.16)	CdWO <sub>4</sub>
$^{130}\text{Te}$	34.5	2.529	4.89	3.0 [231, 232, 239]	ISM, EDF (R)QRPA EDF	0.52, 0.27 (0.25, 0.43) (0.33, 0.46)	CUORE
					ISM, EDF (R)QRPA	0.44, 0.23 (0.17, 0.30)	EXO, NEXT KamLAND-Zen
$^{136}\text{Xe}$	8.9	2.467	5.13	5.7 [40]	EDF (R)QRPA	4.68 (2.13, 2.88)	SuperNEMO SNO+ DCBA
$^{150}\text{Nd}$	5.6	3.368	23.2	0.018 [38, 240]	EDF (R)QRPA	4.68 (2.13, 2.88)	SuperNEMO SNO+ DCBA

# Including Uncertainties in NMEs for $\langle m_{\beta\beta} \rangle = 0.05$ eV

Avignone, Elliott and Engel  
Reviews of Modern Physics, 80 (2008)

Dell’Oro, Marcocci, Viel and Vissani  
Advances in High Energy Physics (2016)

Vergados, Ejiri and Simkovic,  
Rep. Prog. Phys. 75 106301 (2012)



Need to reduce uncertainties in  $0\nu\beta\beta$  decay NMEs !!!